Molecular Therapy
Methods & Clinical Development
Original Article

Preclinical studies in support of phase I/II clinical trials to treat *GUCY2D*-associated Leber congenital amaurosis

Sanford L. Boye,[1] Catherine O'Riordan,[2] James Morris,[2] Michael Lukason,[2] David Compton,[2] Rena Baek,[2] Dana M. Elmore,[3] James.J. Peterson,[3] Diego Fajardo,[3] K. Tyler McCullough,[3] Abraham Scaria,[2] Alison McVie-Wylie,[2] and Shannon E. Boye[4]

[1]Powell Gene Therapy Center, Department of Pediatrics, University of Florida, Gainesville, FL 32610, USA; [2]Sanofi, Framingham, MA 01701, USA; [3]Atsena Therapeutics, Durham, NC 27701, USA; [4]Division of Cellular and Molecular Therapy, Department of Pediatrics, University of Florida, PO Box 100296, Gainesville, FL 32610, USA

Mutations in *GUCY2D* are associated with severe early-onset retinal dystrophy, Leber congenital amaurosis type 1 (LCA1), a leading cause of blindness in children. Despite a high degree of visual disturbance stemming from photoreceptor dysfunction, patients with LCA1 largely retain normal photoreceptor structure, suggesting that they are good candidates for gene replacement therapy. The purpose of this study was to conduct the preclinical and IND-enabling experiments required to support clinical application of AAV5-hGRK1-*GUCY2D* in patients harboring biallelic recessive mutations in *GUCY2D*. Preclinical studies were conducted in mice to evaluate the effect of vector manufacturing platforms and transgene species on the therapeutic response. Dose-ranging studies were conducted in cynomolgus monkeys to establish the minimum dose required for efficient photoreceptor transduction. Good laboratory practice (GLP) studies evaluated systemic biodistribution in rats and toxicology in non-human primates (NHPs). These results expanded our knowledge of dose response for an AAV5-vectored transgene under control of the human rhodopsin kinase (hGRK1) promoter in NHPs with respect to photoreceptor transduction and safety and, in combination with the rat biodistribution and mouse efficacy studies, informed the design of a first-in-human clinical study in patients with LCA1.

INTRODUCTION

Autosomal recessive mutations in *GUCY2D* are associated with Leber congenital amaurosis type 1 (LCA1), a rare childhood blindness that typically presents in the first year of life. There are no disease-modifying treatments currently available for *GUCY2D*-LCA. *GUCY2D* encodes retinal guanylate cyclase (retGC1), a 120-kDa membrane protein responsible for re-synthesis of cyclic guanosine monophosphate (cGMP) required for recovery of the dark-adapted state of photoreceptors after phototransduction. Thus, deficiency in retGC1 creates the biological equivalence of chronic light exposure in rod and cone photoreceptors but without severe degeneration. Despite loss of photoreceptor function, patients with *GUCY2D*-LCA present with a relatively preserved retinal architecture with retention of rods and cones in the macula and peripheral retina into adulthood.[1,2] Magnetic resonance imaging in a small group of adults with *GUCY2D*-LCA1 demonstrated preserved optic chiasm volume and white matter organization of the optic radiations.[3] This disorder is an ideal candidate for a gene therapy approach because there is a long window for therapeutic intervention.

We developed an adeno-associated vector type 5 (AAV5) containing the human *GUCY2D* cDNA under transcriptional control of the photoreceptor-specific human rhodopsin kinase (hGRK1) promoter. AAV5-hGRK1-*GUCY2D* was formulated as a solution for intraocular administration and is being delivered by one-time subretinal injection in an ongoing phase I/II clinical trial (ClinicalTrials.gov: NCT03920007) that is showing early signs of efficacy and safety.[4] This study describes the steps taken to inform the design of this ongoing first-in-human trial. If approved, this gene replacement approach would be a first-in-class treatment for *GUCY2D*-LCA.

RESULTS

The AAV5-hGRK1-based vector expresses a transgene and mediates functional rescue in rod and cone photoreceptors in subretinally injected GCDKO mice

A preclinical study was conducted in guanylate cyclase1/2 double knockout (GCDKO) mice to evaluate transgene expression and, separately, restoration of photoreceptor function after administration of AAV5-hGRK1-based vectors containing GFP and *Gucy2e*, respectively. GCDKO mice were used because they carry disruptions in the *Gucy2e* and *Gucy2f* genes and exhibit loss of rod/cone structure and function and thus serve as a model in which therapeutic effects on both photoreceptor subtypes can be addressed.[5] They also lack

Received 2 August 2022; accepted 12 December 2022;
https://doi.org/10.1016/j.omtm.2022.12.007.

Correspondence: Shannon E. Boye, Division of Cellular and Molecular Therapy, Department of Pediatrics, University of Florida, PO Box 100296, Gainesville, FL 32610, USA.
E-mail: shaire@ufl.edu

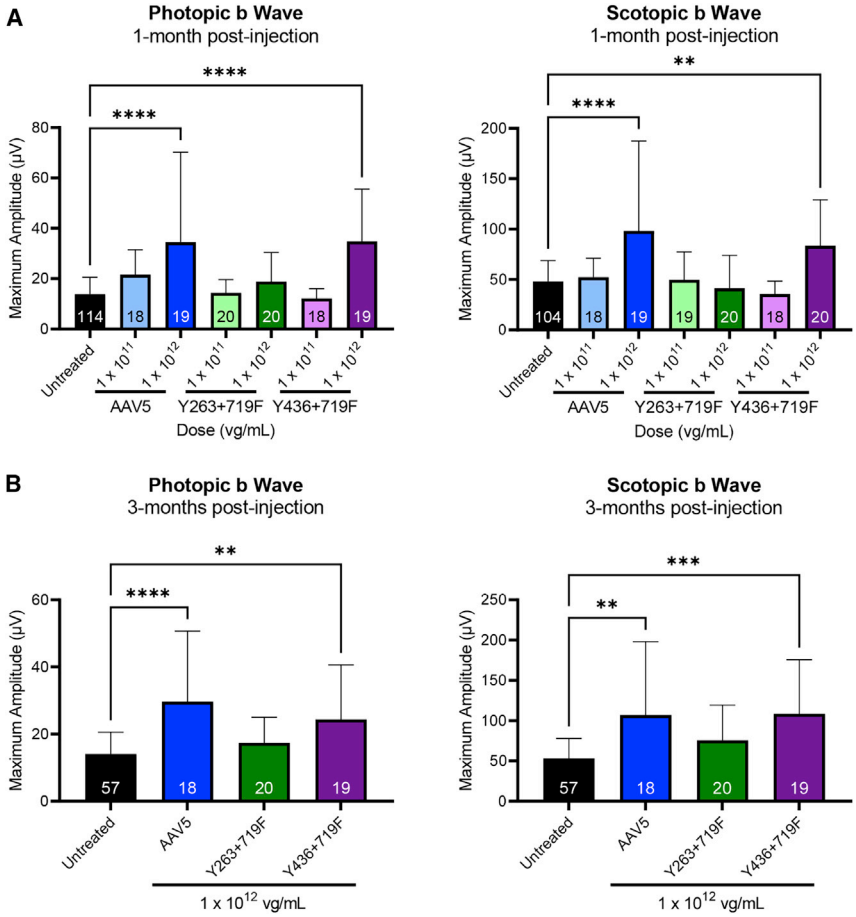

Figure 1. AAV5-based vectors containing hGRK1-Gucy2e significantly improve retinal function in GCDKO mice

(A and B) Cone-mediated (photopic) and rod-mediated (scotopic) function were evaluated in GCDKO mice 1 month (A) and 3 months (B) after subretinal injection with AAV5, AAV5(Y263+719F), or AAV5(Y436+719F) vectors at low (1×10^{11} vg/mL) or high (1×10^{12} vg/mL) concentrations. This corresponds to doses of 1×10^{8} and 1×10^{9} vg/eye, respectively. Animals treated with the high dose of AAV5 or AAV5(Y436+719F) showed sustained and statistically significant increases in photopic and scotopic b waves relative to untreated controls for at least 3 months p.i. (B). There was no significant difference in b wave amplitudes observed between these two vectors at any time point. **$p < 0.01$, ***$p < 0.001$, ****$p < 0.0001$, as determined by one-way ANOVA with Tukey's post-test analysis.

all retinal guanylate cyclase and, thus, have been used to evaluate AAV-mediated guanylate cyclase enzyme activity.[6]

Previous studies have shown that mutations of surface-exposed tyrosine residues led to increased transduction of AAV2, AAV8, and AAV9 *in vitro* and *in vivo*.[7] We therefore created AAV5 variants harboring tyrosine-to-phenylalanine (Y-F) capsid mutations containing a self-complementary smCBA-mCherry genome and tested them along with AAV5 for their relative transduction of an ocular cell line (APRE-19). Based on these results (Figure S1), AAV5 and two AAV5-based capsid mutants were selected to evaluate functional rescue and gene expression *in vivo*. GCDKO mice received a single subretinal administration of AAV5, AAV5(Y263+719F), or AAV5(Y436+719F) containing hGRK1-*Gucy2e* or AAV5-hGRK1-GFP at low (1×10^{11} vector genomes [vg]/mL) or high (1×10^{12} vg/mL) concentration in a volume of 1 μL (corresponding to 1×10^{8} and 1×10^{9} vg/eye, respectively). All vectors were single stranded. Mice were treated between post-natal day 25 (P25) and P35, an age when photoreceptor function (as assessed by electroretinography [ERG]) is absent in untreated mice.[5] The study design is shown in Table S1.

Fundoscopy revealed transgene (GFP) expression after a subretinal administration of AAV5-hGRK1-GFP, AAV5(Y263+719F)-hGRK1-GFP, and AAV5(Y436+719F)-hGRK1-GFP at 1×10^{12} vg/mL (groups 2, 4, and 6, respectively) in GCDKO mice 1 month after injection (Figure S1). None of the mice that received subretinal administration of low-dose vectors (groups 1, 3, and 5, respectively) exhibited any measurable GFP expression. Mice injected with AAV5(Y263+719F)-hGRK1-GFP showed the strongest GFP expression by fundus imaging. However, it was later discovered that this group received a significantly higher vector dose, as measured by titer analysis of dose retains (Table S2). Mice that received AAV5-hGRK1-GFP and AAV5(Y436+719F)-hGRK1-GFP had comparable levels of GFP expression, as measured by fundus imaging (Figure S1).

Significantly increased photopic (cone-mediated) and scotopic (rod-mediated) ERG b wave amplitudes were observed in GCDKO mice 1 month after injection with AAV5-hGRK1-Gucy2e and AAV5(Y436-719F) compared with uninjected controls (Figure 1A). There was an apparent dose response between the two dose levels evaluated. ERG data from animals treated with the highest concentration (1×10^{12} vg/mL, corresponding to a dose of 1×10^{9} vg/eye) showed sustained and statistically significant increases in photopic and scotopic b waves for at least 3 months after injection for AAV5 and AAV5(Y436+719F) (Figure 1B). Mice treated with the lower concentration (1×10^{11} vg/mL) did not show significant improvement relative to untreated controls at any time point. The levels of retinal function in high-dose-treated mice were similar to previously published data that demonstrated that ERG improvements of ~45% were sufficient for full recovery of visually guided behavior (visual acuity and contrast sensitivity).[8] These results demonstrate that an AAV5-hGRK1-based vector expresses the transgene and mediates

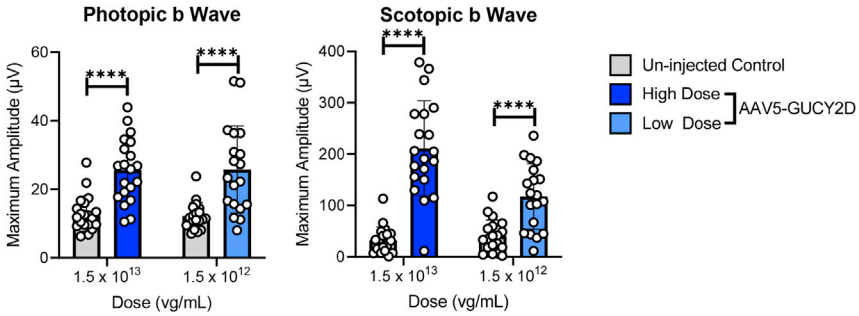

Figure 2. AAV5-hGRK1-GUCY2D significantly improves retinal function in GCDKO mice

Cone-mediated (photopic) and rod-mediated (scotopic) function were evaluated in GCDKO mice 1 month after subretinal injection with vector at low (1.5×10^{12} vg/mL) or high (1×10^{13} vg/mL) concentrations. This corresponds to doses of 1.5×10^{9} and 1×10^{10} vg/eye, respectively. Statistically significant increases in photopic and scotopic b waves relative to untreated controls were observed. ****p > 0.0001, as determined by multiple paired t tests with Holm-Sidak correction for multiple comparisons. n = 19 in the uninjected control groups at low and high doses; n = 20 in the AAV5-GUCY2D treated groups at low and high doses.

functional rescue in rod and cone photoreceptors in GCDKO mice. Because no appreciable difference was observed in responses elicited by AAV5 and AAV5(Y436-719F), the decision was made to proceed with AAV5.

AAV5-hGRK1 containing human GUCY2D is therapeutic in GCDKO mice

Next we evaluated improvements in retinal function after a single subretinal administration of AAV5 expressing the human *GUCY2D* gene in GCDKO mice. Mice received a 1-μL injection of 1.5×10^{12} or 1.5×10^{13} vg/mL of AAV5-hGRK1-*GUCY2D* (corresponding to 1.5×10^{9} and 1.5×10^{10} vg/eye, respectively), and ERG recordings were collected approximately 1 month after injection. The study design is shown in Table S3.

Significantly increased photopic and scotopic b wave amplitudes were observed 1 month after injection with AAV5-hGRK1-*GUCY2D* at 1.5×10^{12} and 1.5×10^{13} vg/mL compared with uninjected controls (Figure 2). Cone responses were not significantly different between the low (1.5×10^{12} vg/mL) and high (1.5×10^{13} vg/mL) concentrations evaluated. Rod-mediated b wave amplitudes demonstrated a statistically significant increase at the high dose compared with the low dose in GCDKO mice. The results of this study show that subretinal delivery of an AAV5-hGRK1 vector containing the human *GUCY2D* coding sequence significantly improves cone and rod function in the GCDKO mouse model of LCA1.

AAV5-hGRK1-GUCYD vectors manufactured via triple transfection or producer cell line restore cone and rod function in GCDKO mice

Because our earlier studies were conducted using a research-quality AAV5 vector manufactured by plasmid triple transfection (TTx), and the clinical manufacturing process used a producer cell line (PCL) approach, we sought to confirm the potency of the PCL material *in vivo*. TTx- and PCL-made material were evaluated and compared after subretinal injection in GCDKO mice. The study design is shown in Table S4. The TTx material used here was a research-grade vector produced at the University of Florida. It was purified by iodixanol step gradient and ion-exchange chromatography.[9] The PCL vector evaluated in this study is the same lot of material evaluated in the good laboratory practice (GLP) non-human primate (NHP) toxicology studies (Tox lot) described below, was made at Sanofi, and was purified by 2-column chromatography where the second column was designed to enrich for full capsids.[10]

The results showed that the PCL-manufactured vector produced a dose-dependent ERG response over the range evaluated (1.5×10^{11} through 1.5×10^{13} vg/mL, corresponding to 1.5×10^{8} through 1.5×10^{10} vg/eye) Figure S2). At a matched concentration of 1.5×10^{12} vg/mL, the PCL material conferred significantly higher ERG responses at some but not all time points after injection relative to the TTx material (Figure 3A). Analytical ultracentrifugation (AUC) analysis of vectors generated using the PCL platform revealed four distinct populations of capsids with sedimentation coefficients of 103S, 90S, 81S, and 64S, with the 64S species representing empty capsids and the 103S species representing capsids containing the full *GUCY2D* vector genome. The x axis represents the sedimentation coefficient in Svedberg units S, and the y axis represents the concentration as a function of S (Figure 3B). The integration of each peak yields the relative concentration of each species in units of detection, and the application of Beer's law (C = A/el) yields the concentration of each species. Molar extinction coefficient values for empty capsids and genome-containing capsids were determined according to Burnham et al.,[11] and the relative percentage of each species was determined. The PCL-made vector contains 5% empty capsids and 81% full-length genome-containing capsids. The 90S and 81S species represent capsids harboring fragmented genomes and represent 10% and 4% of the capsid species, respectively. In contrast the AAV5-GUCY2D vectors generated using the transient transfection AAV production protocol had only 33% of the capsids harboring a full-length vector genome, 102S species, and 45% empty capsids, represented by the 64S species. The 88S and 79S species represent capsids harboring fragmented vector genomes (Figure 3). In addition to the empty-to-full capsid ratio, it is also possible that the different purification methods accounted for the observed differences in ERG responses. The experiments we performed next shed additional light on this concept.

Although mean outer nuclear layer (ONL) thickness in GCDKO eyes treated with the PCL and TTx vector at 1.5×10^{12} vg/mL (1.5×10^{9} vg/eye) was not significantly different from uninjected controls, significant reductions in mean ONL thickness were observed after

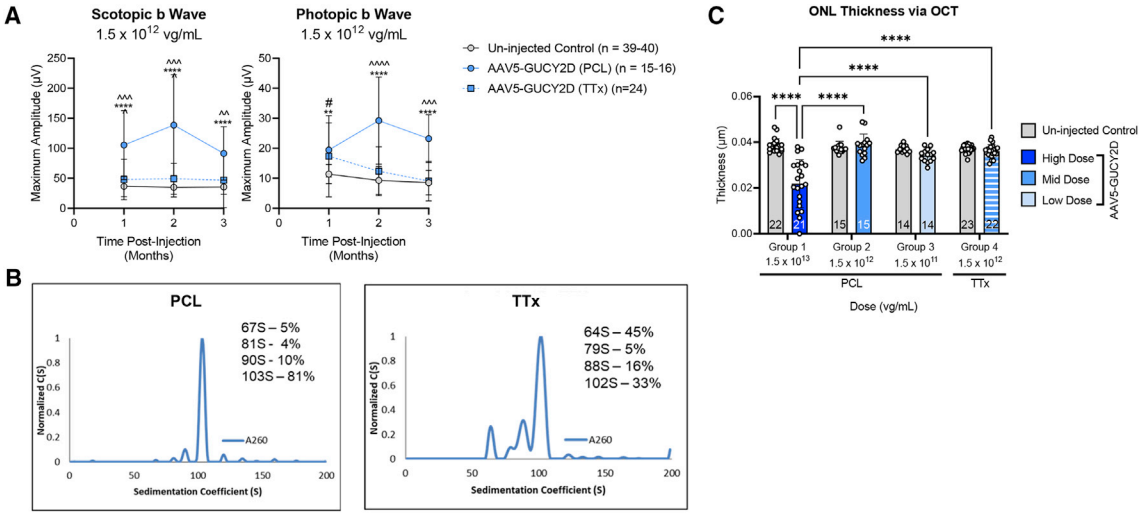

Figure 3. AAV5-hGRK1-GUCY2D produced via PCL or TTx significantly improves retinal function in subretinally injected GCDKO mice

(A) Rod-mediated (scotopic) and cone-mediated (photopic) function were evaluated in GCDKO mice for 3 months after injection with producer cell line (PCL)- or triple transfection (TTx)-made vectors at a matched concentration of 1.5×10^{12} vg/mL. This corresponds to a total dose of 1.5×10^{9} vg/eye. *p < 0.05, **p < 0.01, ***p < 0.001, ****p < 0.0001, PCL versus uninjected Control; ^p < 0.05, ^^p < 0.01, ^^^p < 0.001, ^^^^p < 0.0001, PCL versus TTx; #p < 0.05, ##p < 0.01, ###p < 0.001, ####p < 0.0001, TTx versus uninjected control, as determined by two-way ANOVA with Sidak's post-test analysis. Note than animal numbers measured over the course of the study are presented as a range in the legend. (B) Boundary sedimentation velocity profiles of AAV5 vectors containing the *GUCY2D* vector genome. Analytical ultracentrifugation (AUC) revealed that the PCL-made vector contained 81% full and 5% empty capsids, whereas the TTx-made vector contained 33% full and 45% empty capsids. (C) Mean ONL thickness in GCDKO mouse retinas treated with low- or mid-dose vectors (PCL or TTx made) were not significantly reduced relative to untreated controls. Injection with high-concentration (1×10^{13} vg/mL) PCL-made vector (corresponding to 1×10^{10} vg/eye) resulted in significant retinal thinning in treated animals. **p < 0.01, ***p < 0.001, ****p < 0.0001, as determined by two-way ANOVA with Tukey's post-test.

injection of 1.5×10^{13} vg/mL (1.5×10^{10} vg/eye) of PCL material relative to uninjected controls (Figure 3). The substantial reduction in ONL thickness at the highest concentration tested (1.5×10^{13} vg/mL) indicates an adverse effect on photoreceptors.

A hybrid study evaluates the safety and efficacy of AAV5-hGRK1-GUCY2D in mice

Next we designed a comprehensive dose-ranging study to evaluate the pharmacologically active dose range and determine the minimally effective dose of AAV5-hGRK1-*GUCY2D*. The lot of material used in this study was the same PCL-made lot evaluated in all GLP tox studies (Tox lot). The guanylate cyclase 1 knockout (GC1KO) mouse was selected as the model for this hybrid study because it allows evaluation of safety and efficacy in one setting. GC1KO mice lack cone function, and their cones degenerate. Efficacy can therefore be established via improvements in cone function/structure after treatment via photopic ERG and optical coherence tomography (OCT), respectively. Rod function and structure are retained in GC1KO mice because of the presence of retGC2 (encoded by *Gucy2f*).[5] Safety can therefore be evaluated by any negative effect on function via scotopic (rod) ERG. Because rods make up 95% of photoreceptors in the murine retina, changes in ONL thickness as measured by OCT allow evaluation of retinal photoreceptor health. The hybrid study design is shown in Table S5.

Gross ophthalmic examinations were conducted 3 days, 1 month, and 3 months after injection. All lesions observed in the gross ophthalmic examinations were deemed to be procedurally associated with injection or congenital to the strain background and not the result of the test article.

Cone-mediated retinal function was significantly restored to GC1KO mouse eyes treated with 3.3×10^{11} or 1.5×10^{11} vg/mL of AAV5-*GUCY2D* (Figure 4A). This corresponds to 3.3×10^{8} and 1.5×10^{8} vg/eye, respectively. Although photopic ERG responses were not significantly improved at 3.3×10^{10} vg/mL (3.3×10^{7} vg/eye) relative to uninjected controls, genuine waveforms and photopic ERG responses were measurable in the majority of the AAV5-*GUCY2D* treated eyes at this low dose (Figure 4B). No consistent changes in rod-mediated retinal function were observed with treatment at any dose in this mouse model, nor were reduced scotopic ERG responses observed, suggesting that the AAV5-*GUCY2D* vector did not deleteriously affect rod function at the dose ranges evaluated in this study.

OCT analysis was conducted 3 months post-injection. As expected, the mean ONL thickness in treated eyes of GC1KO mice was modestly reduced relative to uninjected control eyes in all treatment groups, including the vehicle controls. This is a typical finding after subretinal injection in relatively non-degenerative retinas (Figure 4C).[12] There was no significant difference in ONL thickness between vehicle-treated and AAV5-hGRK1-*GUCY2D*-treated eyes at any dose, indicating that the test article was well tolerated (Figure 4C).

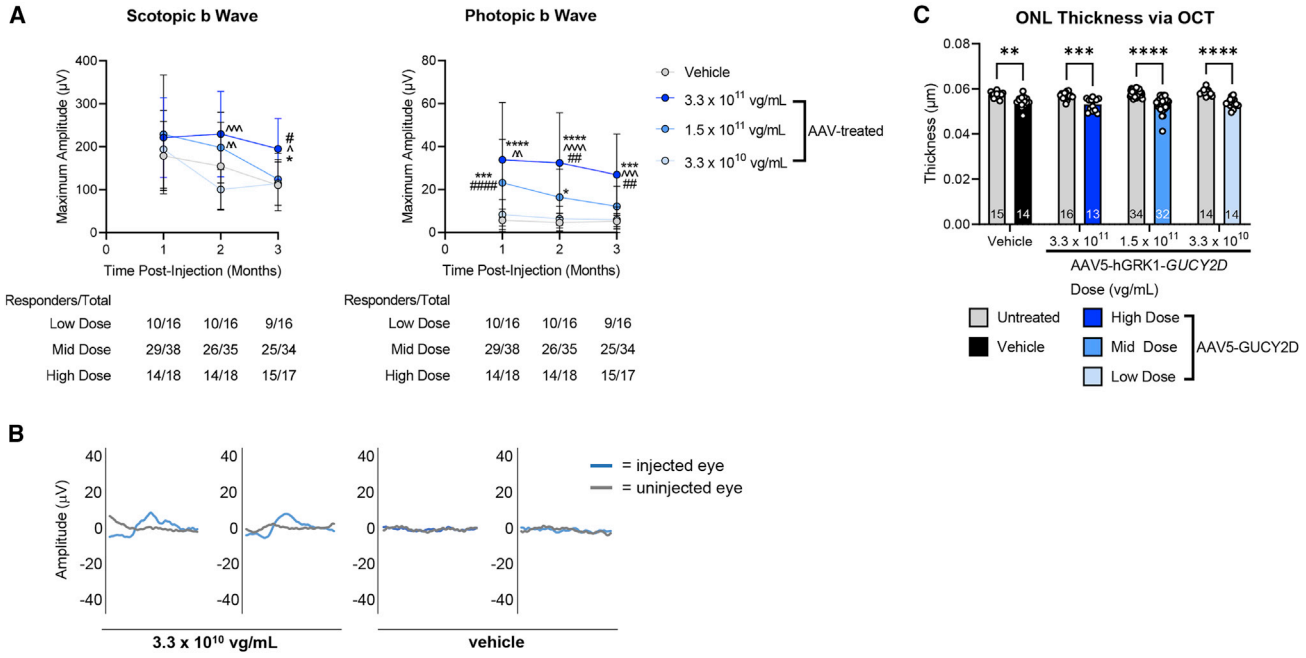

Figure 4. Hybrid study evaluates safety and efficacy of AAV5-hGRK1-GUCY2D in subretinally injected GC1KO mice

(A) Rod-mediated (scotopic) and cone-mediated (photopic) function were evaluated in GCDKO mice for 3 months after injection with a low (3.3×10^{10} vg/mL), mid (1.5×10^{11} vg/mL), or high (3.3×10^{11} vg/mL) concentration of the vector. This corresponds to doses of 3.3×10^{7}, 1.5×10^{8}, and 3.3×10^{8} vg/eye, respectively. (B) Cone mediated b wave amplitudes were significantly improved after treatment with the mid- and high-dose vector. Although significant improvements were not observed at the low dose, genuine waveforms were present in the majority (9 of 16) of treated animals. Two representative waveforms from low-dose vector-treated and vehicle-treated mice reflect this observation. *p < 0.05, **p < 0.01, ***p < 0.001, ****p < 0.0001 versus vehicle; ^p < 0.05, ^^p < 0.01, ^^^p < 0.001, ^^^^p < 0.0001 versus low dose; #p < 0.05, ##p < 0.01, ###p < 0.001, ####p < 0.0001 versus mid dose, as determined by two-way ANOVA with Tukey's post-test analysis. (C) There was no significant difference in mean outer nuclear layer (ONL) thickness between vehicle-treated and AAV5-hGRK1-*GUCY2D*-treated eyes at any dose, indicating that the test article was well tolerated. **p < 0.01, ***p < 0.001, ****p < 0.0001, as determined by two-way ANOVA with Tukey's post-test analysis.

Histopathology analysis was conducted on animals at the end of the study (3 months after injection). Dose-related microscopic findings were observed in the outer layers of the retina in the mid-dose (1.5×10^{11} vg/mL) and high-dose (3.3×10^{11} vg/mL) cohorts. These changes were identified at the microscopic level and were not observable by OCT. They were characterized by focal/multifocal loss of photoreceptors together with secondary disorganization of the inner plexiform and inner nuclear layers. There was no evidence of loss of function (as measured by ERG) or test article-related loss of photoreceptors across the retina as a function of dose (as measured by OCT). Other retinal findings were regarded as incidental to the injection procedure and resolution of the associated retinal separation from the retinal pigmented epithelium.

Comparing the therapeutic response to AAVs containing the murine Gucy2e versus human GUCY2D coding sequence

To determine whether a different therapeutic response could be observed after subretinal administration of AAV5-*GUCY2D* (human gene) or AAV5-*Gucy2e* (mouse gene), an exploratory study was conducted in GC1KO mice. The study design is shown in Table S6. The mouse *Gucy2e* and human *GUCY2D* vectors were prepared by TTx by Sanofi, utilizing the same downstream purification methodology as the GLP vector. This was done to eliminate potential differences in results because of manufacture of the test article. Both vectors were purified similarly via 2-column chromatography.[10]

The results showed that both vectors demonstrated dose-responsive restoration in cone photoreceptor function. There were no consistent differences between AAV5-*GUCY2D* versus AAV5-*Gucy2e* at any equivalent dose or time point (Figure 5A). A summary of all statistical comparisons across photopic amplitudes 1, 2, and 3 months post injection (p.i.) are presented in Tables S7–S9. Statistical comparisons of scotopic amplitudes 1 month p.i. are shown in Table S10. By 2 months p.i., there were no statistically significant differences in scotopic amplitudes across groups. Analysis of retinal structure revealed no difference in mean ONL thickness in GC1KO mice treated with AAV5-*GUCY2D* or AAV5-*Gucy2e* eyes at any dose (Figure 5C). Visually guided behavior was improved in mice treated with either vector to almost wild-type levels, even at the lowest dose evaluated (3.3×10^{10} vg/mL) (Figure 5D).

Another notable finding from this experiment relates to vector manufacturing and purification on potency. We found that the potency of the TTx-made vector was similar to that of the PCL-made

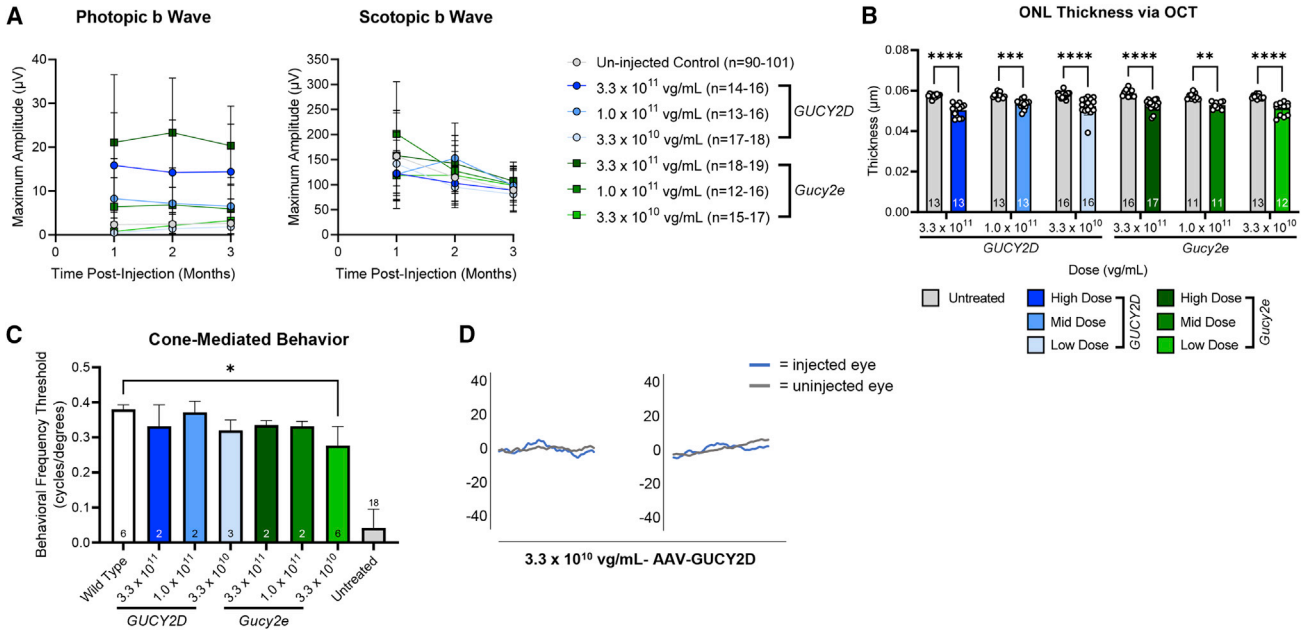

Figure 5. AAV5 vectors containing the human *GUCY2D* or murine *Gucy2e* coding sequence, manufactured via TTx, and purified via 2 CC confer significant improvements in retinal function to GC1KO mice

(A) The AAV-*GUCY2D* and AAV5-*Gucy2e* vectors demonstrated stable and dose-responsive restoration of cone PR function for at least 3 months after injection. There were no significant differences in photopic b wave amplitudes between AAV5-*GUCY2D*- versus AAV5-*Gucy2e*-treated eyes at any equivalent dose or time point. By 2 months p.i., there were no significant differences in scotopic b wave amplitudes. A summary of all statistical comparisons can be found in Figures S7–S10. (B) No significant difference in mean ONL thickness was observed across treatment groups. $^{**}p < 0.01$, $^{***}p < 0.001$, $^{****}p < 0.0001$, as determined by two-way ANOVA with Tukey's post-test analysis. (C) Two representative photopic (cone-mediated) ERG waveforms from mice treated with 3.3×10^{10} vg/mL (3.3×10^{7} vg/eye) of AAV5-GUCY2D were made via TTx and purified via 2-column chromatography (2 CC). (D) Despite the barely visible ERG waveforms, these mice had near-normal cone-mediated behavior.

AAV5-*GUCY2D* vector when both were purified via the same 2-column chromatography (2 CC) method. In this experiment (Figure 5; Table S7), and in the prior experiment employing PCL-made AAV-*GUCY2D* (Figure 4), the minimum dose to elicit statistically significant improvements in cone ERG amplitudes 1 month p.i. was similar: 1.0×10^{11} vg/mL for TTx and 1.5×10^{11} vg/mL for PCL. As with the PCL-made vector, we observed genuine photopic (cone-mediated) waveforms after treatment at the low dose (3.3×10^{10} vg/mL) of TTx-made AAV-*GUCY2D* (Figure 5B). This contrasts our findings shown in Figure 3, where vector made via PCL/purified via 2 CC was more potent than the TTx-made vector purified via iodixanol step gradient/ion-exchange chromatography. AUC analysis revealed that vectors used in this experiment (Figure 5) contained a high proportion (>90%) of full capsid particles (data not shown). These results indicate that the purification approach and empty capsid burden, among other things, can affect vector potency *in vivo*.

Evaluation of photoreceptor transduction in NHPs using AAV5-hGRK1-GFP

Next, a non-GLP study was conducted in NHPs to evaluate GFP expression in photoreceptors after subretinal administration of AAV5-hGRK1-GFP. We have shown previously that subretinal delivery of AAV5-GRK1-GFP results in transgene expression limited exclusively to photoreceptors.[13] The cynomolgus monkey was selected for this study because the NHP eye is the only commonly used nonclinical species with a macula and fovea similar to that of the human eye. We observed a clear dose-dependent increase in photoreceptor transduction in NHP eyes over the dose range evaluated (1.0×10^{10}–1.0×10^{12} vg/mL). A dose response in total photoreceptor transduction was observed after a single subretinal administration of AAV5-hGRK1-EGFP in NHPs. A summary of photoreceptor transduction in the NHP studies is provided in Table S11. Average and peak photoreceptor transduction across all eyes are reported.

At the lowest dose (1.0×10^{10} vg/mL), approximately 4% of photoreceptors were GFP positive, whereas at the mid-dose (1.0×10^{11} vg/mL) and high dose (1.0×10^{12} vg/mL), 22% and 94% of photoreceptors were GFP positive, respectively. At 3.3×10^{11} vg/mL, 91% of photoreceptors were GFP positive, indicating that transduction was only marginally improved at higher concentrations. The subretinal injection was initiated in the area of the retina in the temporal arcades. The resulting bleb included the macula region as well as the fovea and accounted for approximately 10%–15% of the retinal surface area. This area is desirable for correction in the eye of a patient with LCA1 because it includes the cone photoreceptor-rich region of the retina responsible for central vision. Photoreceptor transduction remained within the borders of the bleb, and little to no transduction

Table 1. Design of the 9-month NHP GLP toxicology study to evaluate safety and determine the BD of AAV5-hGRK1-*GUCY2D* in cynomolgus monkeys

Group[a]	No. of animals[b]		Dosing regimen[c]		Dose level[d] (vg/eye)	Dose concentration (vg/mL)
	Male	Female	Right eye	Left eye		
1	4	4	vehicle	not dosed	0	0
2	4	4	test article	not dosed	1.5×10^{11}	1.0×10^{12}
3	4	4	test article	not dosed	6.0×10^{11}	4.0×10^{12}
4//7[e]	3	5	test article	not dosed	1.5×10^{12}	1.0×10^{13}
5	4	4	test article	not dosed	7.4×10^{12}	4.9×10^{13}

Male and female cynomolgus monkeys (*M. fascicularis*) were assigned to five groups, and doses were administered as indicated. Animals were dosed via subretinal injection to the right eye once on day 1 of the dosing phase at a volume of 150 μL. The vehicle control article/diluent was Alcon BSS with 0.014% polysorbate 20. Assessment of toxicity was based on mortality, clinical observations, body weight, food consumption, ophthalmic observations, intraocular pressure (IOP) measurements, optical coherence tomography (OCT), full-field electroretinography (ffERG), multi-focal electroretinography (mfERG), and clinical and anatomic pathology. Fundus ocular photography was performed for documentation purposes only. Blood samples were collected to determine BD of the test article, expression of the transgene, cellular immune response, and immunogenicity. Aqueous humor was collected to determine immunogenicity. Frozen tissue samples were collected at the 1-month necropsy to determine BD of the test article and expression of the transgene.

[a]Group 1 received the vehicle control article only.

[b]Cohorts were designated as follows (survival permitting). Cohort 1 was two males/group and designated for the 9-month terminal sacrifice. Cohort 2 was two females/group and designated for the 9-month terminal sacrifice. Cohort 3 was two males/group and designated for the 1-month interim sacrifice, with the exception of group 4, which had one male. Cohort 4 was two females/group and designated for the 1-month interim sacrifice, with the exception of group 4, which had three females. Each cohort was designated as a subgroup in the data collection system (Pristima).

[c]Two animals/sex/group were designated for interim necropsy 1 month after dosing. The remaining animals were designated for terminal necropsy, 9 months after dosing.

[d]Dose levels were based on the test article as supplied. The right eye of each animal was dosed at a volume of 150 μL.

[e]Because of unscheduled euthanasia of a group 4 male on day 1, a replacement female was added to the study.

was observed outside of the bleb edge. Figure S3 shows a schematic of how images were collected, an example image showing photoreceptor transduction within the subretinal injection bleb, and an example of how quantification was performed to arrive at the results highlighted in Table S11.

GLP safety studies in rats and NHPs establish 1×10^{12} vg/mL as the "no observable adverse effect" level

We evaluated the safety of AAV5-*GUCY2D* in a GLP rat biodistribution (BD) study and two GLP safety studies performed in cynomolgus monkeys. For scaling of dose between species, we utilized the convention established in previous preclinical studies evaluating the safety of AAV2-*RPE65*.[14–16] Dose is increased by increasing the concentration of the vector. The volume of vector delivered is scaled based on the respective eye size and surgical considerations inherent to performing subretinal injection in each species. Specifically, the maximum practical volume that can be delivered by transvitreal subretinal injection to the mouse eye is 1 μL, which leads to approximately 60%–80% coverage of the retina. In macaques (and dogs), the maximum volume that can be delivered without performing vitrectomy and paracentesis is 150 μL. When placed centrally in a macaque retina, 150 μL is sufficient to create a bleb encompassing the entire macula, which is the target area of treatment in LCA1.

The GLP rat BD study evaluated two different doses of AAV5-*GUCY2D* (Table S12). GLP NHP study 1 was longer in duration (1–9 months) and focused on BD and toxicity at relatively high doses of the test article that were administered without steroid prophylaxis (Table 1). GLP NHP study 2 was shorter in duration (3 months) and focused on ocular toxicity at lower doses of the test article that were administered with steroid prophylaxis (Table 2).

BD of AAV5-GUCY2D following subretinal administration

In the rat BD study, two different doses of vector, low (1.0×10^{12} vg/mL, 2.0×10^{9} vg) and high (1.0×10^{13} vg/mL, 2.0×10^{10} vg), were injected subretinally into adult Long Evans rats in a volume of 2 μL. A panel of tissues was collected at different time points ranging from 3–92 days p.i. (Table S12). Total DNA was extracted, and vector genomes were quantified by quantitative PCR (qPCR) using primers targeted to a region including 5′ *GUCY2D* extending into the bGH poly(A). Tissue samples found to be positive for vector genomes underwent RNA extraction and were then subjected to qRT-PCR to determine the level of vector specific transgene expression. As expected, the highest level of vector DNA was detected in the injected eye, with lower vector DNA levels detected in the optic nerve and brain (Tables S13 and S14). In general, vector DNA in tissue and fluids was greater in the high-dose animals compared with the low dose animals, and the vector DNA levels were greater during earlier time points, indicating that detection of AAV5-*GUCY2D* vector was dose dependent and progressively decreased over time. Vector DNA was only detectable in the blood on day 4 in the high-dose group. Significantly lower, transient levels of vector DNA were detected in 8 of 10 peripheral tissues in the low-dose and 10 of 10 peripheral tissues in the high-dose groups evaluated on day 4. By day 92, 2 of 10 peripheral tissues in the low-dose and 3 of 10 peripheral tissues in the high-dose groups had detectable levels of vector genomes. In the low-dose group, ovaries and testes were positive for vector genomes in 3 of 5 and 1 of 5 animals, respectively, on day 4 and negative for vector genomes on days 15 and 29 (not tested on day 92). In the high-dose group, ovaries and testes were positive for vector genomes in 5 of 5 and 2 of 5 animals, respectively, on day 4. Although a few animals were positive for vector genomes on days 15 and 29, all animals were negative for vector genomes in ovaries

Table 2. Design of the 3-month NHP GLP toxicology study to evaluate safety and determine the BD of AAV5-hGRK1-*GUCY2D*

Group[a,b]	No. of females	Systemic steroid (through dosing phase interval)[c]	Dosing regimen		Dose level (vg/eye)[d]		Dose concentration (vg/mL)	
			Left eye	Right eye	Left eye	Right eye	Left eye	Right eye
1 (control)	3	week 6	not dosed	vehicle	N/A	0	N/A	0
2	3	week 6	not dosed	test article	N/A	1.5×10^{10}	N/A	1.0×10^{11}
3	3	week 6	not dosed	test article	N/A	5.0×10^{10}	N/A	3.3×10^{11}
4	3	week 6	not dosed	test article	N/A	1.5×10^{11}	N/A	1.0×10^{12}
5 (control)	3	day 3	not dosed	vehicle	N/A	0	N/A	0
6	3	day 3	not dosed	test article	N/A	1.5×10^{10}	N/A	1.0×10^{11}
7	3	day 3	not dosed	test article	N/A	5.0×10^{10}	N/A	3.3×10^{11}
8	3	day 3	not dosed	test article	N/A	1.5×10^{11}	N/A	1.0×10^{12}

N/A, not applicable.

Female cynomolgus monkeys (*M. fascicularis*) were assigned to eight groups, and doses were administered as indicated. Animals were dosed once on day 1 of the dosing phase via subretinal injection into the right eye at a volume of 150 μL/right eye. The vehicle control article/diluent was Alcon BSS with 0.014% polysorbate 20. Assessment of toxicity was based on mortality, clinical observations, body weight, body weight change, food consumption, ophthalmic observations, intraocular pressure (IOP), optical coherence tomography (OCT), color fundus photography, full-field and multifocal electroretinography (ffERG and mfERG, respectively), and clinical and anatomical pathology. Blood and aqueous humor samples were collected for immunogenicity analysis.

[a]Groups 1 and 5 received the vehicle control article only.

[b]Animals in all groups (1–8) received subconjunctival dexamethasone (DEX; 2 mg) on day 1 as a routine component of the subretinal procedure, with DEX administered after test article injection.

[c]Animals in groups 1–4 were administered systemic prednisolone (via oral administration) beginning 3 days prior to dosing and continuing through week 6 of the dosing phase in addition to the standard topical DEX as part of the medication regimen. Animals in groups 5–8 were administered systemic prednisolone (via oral administration) beginning 1 day prior to dosing and continuing through day 3 of the dosing phase in addition to the standard topical DEX as part of the medication regimen.

[d]Dose levels were based on the test article as supplied. The right eye of each animal was dosed at a volume of 150 μL.

and testes on day 92. Most of the animals (all but 1 animal in the low-dose group) had documented observations of procedurally related vitreous and/or subretinal hemorrhage in the injected eye immediately after the subretinal procedure, and this may have contributed to systemic distribution of the vector. No non-target tissues were positive for *GUCY2D* transgene expression (based on qRT-PCR), consistent with use of a photoreceptor-specific promoter (hGRK1) in our vector.

Based on the results of the GLP rat BD, select tissues were evaluated for the presence of *GUCY2D* mRNA in GLP NHP safety study 1 (Table 1). In the subretinal injection bleb, similar levels (millions of copies) of *GUCY2D* mRNA were found across each treated group (Table S15). The quantity of *GUCY2D* mRNA expressed in the non-bleb area was several orders of magnitude lower than in the bleb and was not detected in several non-bleb areas. AAV5-*GUCY2D* vector genome DNA was detected in select systemic tissues (brain, optic nerve, spleen, and liver) and blood (Table S16). However, only a single sample from the liver of an animal dosed with the highest dose (4.9×10^{13} vg/mL) was positive for *GUCY2D* mRNA. This provided further evidence that the photoreceptor-specific hGRK1 promoter regulating *GUCY2D* expression was highly effective at restricting expression to the desired cell type, even at these relatively high doses of vector.

Immunological response to subretinal administration of AAV5-GUCY2D

In GLP NHP safety study 1, anti-AAV5 antibodies were observed in the serum of the majority of treated animals by 5 weeks p.i., with all animals demonstrating measurable titers by week 9 (Table S17). In general, serum titer values increased from week 2 to week 13, when they reached a plateau and persisted until the end of the study. Although individual serum titer values varied, in general, titer results were dose dependent and increased with increasing dose concentrations. Anti-AAV5 antibodies were observed in aqueous humor of treated eyes of all animals at the interim and terminal sacrifice (Table S17). In general, mean anti-AAV5 antibody titers in aqueous humor were higher at the higher dose levels, although titer values varied considerably between individual animals in the same treatment group. A single serum sample at week 39 (with a minimal titer of 100) was found to be positive for antibodies directed against the transgene product in an animal administered the highest dose (4.9×10^{13} vg/mL). Otherwise, all remaining post-dose serum and aqueous humor samples were found to be negative for antibodies directed against the transgene product. Subretinal administration of AAV5-*GUCY2D* had no apparent effects on cellular immune response (assessed by ELISpot), body weight, clinical pathology, or macroscopic observations.

Summary of findings from GLP NHP safety study 1

Male and female cynomolgus monkeys were administered the vehicle control article or a dose level of 1.5×10^{11}, 6.0×10^{11}, 1.5×10^{12}, or 7.4×10^{12} vg/eye via subretinal injection and monitored for up to 9 months p.i.. Test article-related adverse findings to the retina were appreciated at all dose levels in a dose-dependent manner. Adverse retinal findings appreciated via OCT included an absent bacillary layer, thinned or absent ONL, choroidal disorganization,

persistent hyper-reflective foci, chorioretinal atrophy, perivascular sheathing, and retinal nerve fiber layer thickening. The OCT retinal findings had adverse microscopic correlates of retinal degeneration/loss (disorganization, thinning, and/or loss of the photoreceptors, ONL, outer plexiform layer, and occasionally the inner nuclear layer), necrosis/loss of retinal pigment epithelium cells, decreased pigmentation in the remaining retinal pigment epithelium (RPE) cells, mononuclear cell inflammation, and vitreous exudate. The OCT and microscopic retinal findings correlated with marked depression of retinal function by week 38, as assessed by full-field and multi-focal ERG. Based on adverse retinal degeneration and corresponding deficits in retinal function, none of the dose levels evaluated in this study were considered to have been tolerated, and a "no observed adverse effect level" (NOAEL) was not established. A full description of the findings from this study can be found in the supplemental information.

GLP NHP safety study 2 identifies NOAEL and a systemic steroid regimen

Despite a favorable systemic safety profile, adverse ocular findings in the initial safety study resulted in failure to identify an NOAEL and prompted a second GLP tox study in cynomolgus macaques. In this study, we evaluated the effect of relatively lower doses (1.0×10^{11} to 1×10^{12} vg/mL) together with two different systemic steroid regimens on the development of ophthalmic inflammation and other findings. A short course of steroids has become standard practice for intraocular delivery of AAV gene therapy vectors.[17] We chose to evaluate two different regimens. Half of the animals (those assigned to groups 1–4) were administered an extended steroid regimen consisting of oral prednisolone (1 mg/kg/day) once daily starting 3 days prior to dosing and continuing for 5 weeks after dosing and then every other day for another week. Those assigned to groups 5–8 were administered oral prednisolone (1 mg/kg/day) the day prior to dosing and through day 3. The study design is outlined in Table 2.

No test article-related effects were noted on clinical observations, body weight, intraocular pressure (IOP), full-field ERG (ffERG), multifocal ERG (mfERG), clinical pathology parameters, or macroscopic observations. No apparent differences with regard to ophthalmic inflammation or any other parameter were noted between animals that received an extended systemic steroid regimen versus those that received the more modest, short-term regimen. Findings considered related to the subretinal dosing procedure were observed in all groups, including controls, and were evident upon ophthalmic examination, color fundus imaging, OCT scanning, and microscopic evaluation.

Findings of note involved the presence of gray-white foci subretinal to the choroid that were observed by ophthalmic examinations (OEs) and fundus photography in the original bleb and/or the surrounding pigment ring, beginning approximately 8 weeks after dosing and continuing through the dosing phase. These foci were also observed by OCT as hyper-reflective foci (HFs) and were also noted away from the bleb edge or injection site of vector-treated eyes (all doses). These white spots and patches were more prevalent superiorly in vector-treated animals (all doses) and associated with RPE and/or photoreceptor (PR) disorganization and/or intraretinal HFs in the PR layers and choroid. Microscopically they were characterized as inflammatory mononuclear infiltrates. Observation of these foci generally scaled with dose. Anterior chamber inflammation was mild to moderate but resolved quickly (before day 22 in all eyes but one). Vitreous inflammation was more pronounced, with cell scores initially moderately severe to severe before rapidly decreasing to mild levels as soon as day 36 in most eyes and in all eyes by day 92. No apparent difference was noted between animals receiving the moderate or minimal steroid regimen. At all dose levels, the inflammatory findings in some animals (those with gray-white foci at OE and correlating with other parameters) were considered immune-mediated based on their corresponding positive anti-AAV5 results. These ophthalmological findings were considered non-adverse because they were transient (inflammation) and/or had no apparent effect on animal health or retinal function (based on ERG). Similar findings after subretinal administration of AAV vectors have been reported previously.[18,19] Thus, the NOAEL was established to be 1.0×10^{12} vg/mL combined with administration of a mild or moderate systemic steroid regimen.

Evaluating comparability between Tox lot versus GMP test articles in GC1KO mice

As part of the evaluation to establish comparability between the GMP material (GMP lot) and the lot used in the GLP tox studies (Tox lot), a non-GLP bridging study was conducted to evaluate the effects of AAV5-*GUCY2D* on PR function and retinal structure. The Tox lot AAV5-*GUCY2D* vector evaluated in previous preclinical studies and in the cynomolgus monkey GLP tox studies and the GMP manufactured material were evaluated in subretinally injected GC1KO mice according to the study design shown in Table S18.

Photopic and scotopic ERG were analyzed 1 month p.i. after subretinal administration of AAV5-*GUCY2D*. Cone-mediated retinal function was significantly restored to GC1KO mouse eyes treated with the Tox lot or GMP lot at 1.5×10^{11} (Figure 6). Although photopic ERG responses were not significantly improved at the 3.3×10^{10} vg/mL dose concentration relative to uninjected controls for both lots, genuine waveforms and photopic ERG responses were measurable in some of the treated eyes. The magnitude and number of responders was similar between the two lots of material evaluated at this dose level. A small but significant increase in photopic ERG response was observed in mice treated with the GMP lot compared with the Tox lot at 1.5×10^{11} vg/mL (Figure 6). Despite this difference in photopic ERG response at the high-dose level, there was no difference in mean ONL thickness in GC1KO eyes treated with the Tox or GMP lots of AAV5-*GUCY2D* (at matched doses) or in the scotopic ERG response at either dose level evaluated (Figure 6).

For full summary of all *in vivo* studies, including the number of animals dosed, the amount of vector injected, and the statistical analyses used to evaluate data, refer to Table S20.

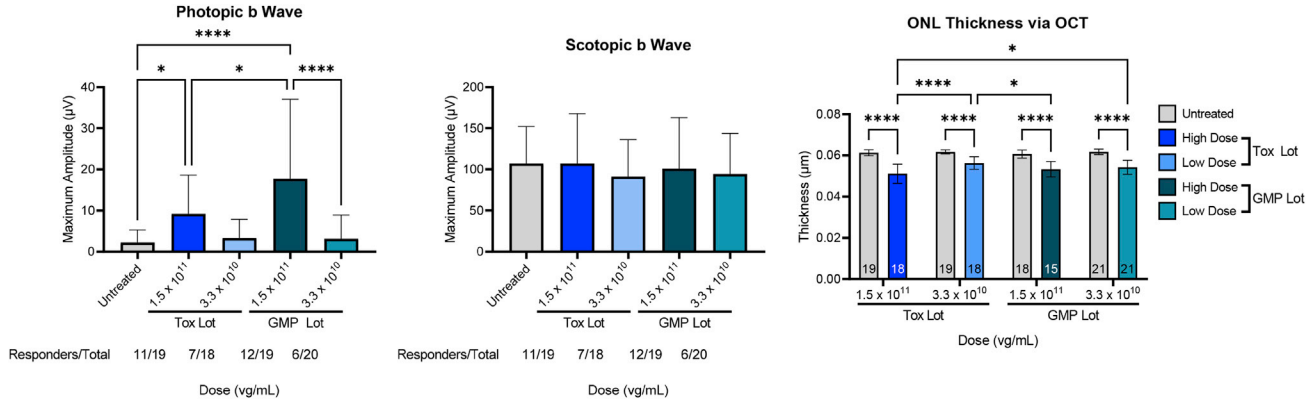

Figure 6. Comparison of retinal structure and function in GC1KO mice treated with the GMP vector versus the vector used in GLP tox studies 1 month p.i.
Photopic b wave amplitudes were significantly higher in GC1KO mouse eyes treated with 1.5×10^{11} vg/mL (1.5×10^{8} vg/eye) of AAV5-GUCY2D (relative to untreated controls), regardless of whether treatment was performed with GMP or Tox lots. At a lower dose of 3.3×10^{10} vg/mL (3.3×10^{7} vg/eye), photopic improvements were not significant, but genuine waveforms were observed in a similar number of animals treated with the GMP lot (6 of 20) and Tox lot (7 of 18) vectors (left). No significant improvements in scotopic b wave amplitudes were observed in vector-treated eyes (center). *$p < 0.05$, ****$p < 0.0001$ as determined by one-way ANOVA with Tukey's post-test analysis. No significant difference in mean ONL thickness was observed in mice treated with the GMP versus Tox lot vector (right). **$p < 0.01$, ***$p < 0.001$, ****$p < 0.0001$, as determined by two-way ANOVA with Tukey's post-test analysis.

DISCUSSION

We document a number of preclinical studies performed in support of a phase I/II trial for LCA caused by biallelic mutations in *GUCY2D*. These studies informed multiple aspects of our path to clinical trial, including choice of AAV capsid, vector dose, and steroid regimen. They also shed light on the relationship between manufacturing and vector quality attributes.

First we focused on the capsid. Our previous work showed that AAV5 efficiently delivered *Gucy2e* to rod and cone PRs and conferred restoration of retinal structure/function and visually guided behavior to mouse models of LCA1.[8,20] With a goal of increasing efficiency of gene delivery, we wanted to determine whether the potency of AAV5, like AAV2, AAV8, and AAV9,[7] could be improved via incorporation of surface-exposed tyrosine mutations. After prescreening multiple AAV5-based Y-F mutant capsid variants *in vitro*, three were tested for their ability to confer therapy in GCDKO mice. Sustained and significant improvements in rod- and cone-mediated ERG were observed for AAV5 and AAV5(Y436+719F), but no appreciable difference in potency was observed between the two capsids. Therefore, the decision was made to proceed with AAV5. AAV5 is also being used in clinical studies targeting other PR-mediated diseases (ClinicalTrials.gov: NCT04671433, *RPGR*-XLRP; ClinicalTrials.gov: NCT03328130, *PDE6B* RP).

Next we focused on vector dose. As done before in other preclinical studies employing subretinal injection across multiple species, we scaled dose by changing vector concentration while adjusting the volume administered in each species based on consideration of eye size and practical limitations.[14–16] Mice received 1 μL and macaques received 150 μL. Results across all mouse studies demonstrated dose-responsive restoration of retinal function after treatment with AAV5-*GUCY2D*, as measured by ERG at all dose levels, and established a pharmacologically active dose range of 3.3×10^{10} to 1.5×10^{13} vg/mL. A decrease in ONL thickness was observed at the highest dose tested, indicating a potential adverse effect at this dose level (1.5×10^{13} vg/mL). The lowest dose evaluated (3.3×10^{10} vg/mL) demonstrated minimal, but measurable, pharmacological activity (measurable ERG responses and clear improvements in visually guided behavior) and is therefore considered the minimal active dose. In agreement with the mouse data, subretinal injection of a surrogate vector, AAV5-hGRK1-GFP, at this dose in macaques led to transduction of 5% of PRs (rods and cones) in the bleb. At a dose 1 log higher (3.3×10^{11} vg/mL), profound retinal transduction (91%) was observed. Increasing the dose further did not lead to higher levels of transduction (Table S11). Of the two NHP GLP tox studies performed, the second utilized relatively lower doses (1.0×10^{11} to 1×10^{12} vg/mL) and a steroid regimen. These studies identified the NOAEL to be 1×10^{12} vg/mL. Based on the collective results in mouse models, non-GLP NHP studies utilizing surrogate AAV5-hGRK1-GFP, and GLP tox studies in NHPs, the starting dose chosen for phase I/II clinical trials was 3.3×10^{10} vg/mL, with a mid dose of 1.0×10^{11} vg/mL and a final high dose of 3.3×10^{11} vg/mL. The mid dose (1×10^{11} vg/mL) and high dose (3.3×10^{11} vg/mL) elicited significant improvements in retinal structure/function and visually guided behavior in mice and transduced up to 22% and 91% of NHP PRs in the bleb, respectively. The high dose selected is three times below the NOAEL identified in NHP GLP tox studies, providing an additional window for dose escalation.

Finally, we focused on steroid regimen. Across two GLP tox studies in NHPs, three different strategies were tested. First, a 9-month study focused on BD and toxicity at relatively high doses was conducted without steroid prophylaxis. The failure to identify an NOAEL in

this study was perhaps unsurprising, given the combination of high vector doses (ranging from 1.0×10^{12} to 4.9×10^{13} vg/mL) and the lack of steroids. Notable findings in these animals, however, related to safety outside of the eye. Systemic toxicity was not observed in NHPs administered doses as high as 150 μL of 4.9×10^{13} vg/mL (7.4×10^{12} vg), nor was expression of the transgene observed outside of ocular tissues. Both findings highlight the value of the PR-specific hGRK1 promoter that was incorporated in the vector construct. Next, a 3-month study focused on ocular toxicity at lower doses (1.0×10^{11} to 1×10^{12} vg/mL) was performed using two different regimens (minimal and mild). The minimal regimen involved systemic prednisolone (via oral administration) beginning 1 day prior to dosing and continuing through day 3 of the dosing phase in addition to the standard topical dexamethasone as part of the medication regimen. The mild regimen involved systemic prednisolone (via oral administration) beginning 3 days prior to dosing and continuing through week 6 of the dosing phase in addition to the standard topical dexamethasone as part of the medication regimen. Ocular toxicity was mitigated with a minimal and moderate steroid regimen. Prophylaxis steroids are now standard in intraocular delivery of AAV gene therapies in clinical studies as well as for the approved ocular gene therapy, Luxturna. For these reasons, we chose to incorporate oral prednisone (1 mg/kg up to 80 mg) daily starting the day before surgery through the second day after surgery and prednisolone 1% and trimethoprim and polymyxin B drops administered to the study eye four times per day starting the day after surgery through day 9 into the phase I/II trial design.

The completed nonclinical studies supported evaluation of AAV5-*GUCY2D* in patients with *GUCY2D*-LCA. Patients in cohort 1 of the ongoing phase I/II clinical trial (ClinicalTrials.gov: NCT03920007) were subretinally injected with 300 μL of 3.3×10^{10} vg/mL, the minimal active dose concentration in the preclinical studies. Subjects have shown clear signs of improved retinal function at the level of best corrected visual acuity (BCVA) and full-field stimulus testing (FST) and an excellent safety profile.[4] Evaluation of these patients and those treated at the mid (1.0×10^{11} vg/mL) and high (3.3×10^{11} vg/mL) doses is ongoing.

MATERIALS AND METHODS

AAV plasmid construction, vector production, and titering

AAV vectors were produced via transient transfection[10] or the PCL method.[21,22] The recombinant AAV vector plasmids contain flanking AAV2 inverted terminal repeats, the human rhodopsin kinase promoter, a splicing signal derived from SV40, human *GUCY2D* or murine *Gucy2e*, and a bovine growth hormone polyadenylation signal.[6,23] AAV5-*GUCY2D* and AAV5-*Gucy2e* vectors were manufactured at the University of Florida using plasmid TTx into HEK293 cells and purification by iodixanol step gradient followed by anion-exchange chromatography and buffer exchange into balanced salt solution (BSS) supplemented with 0.014% Tween 20, according to methods described previously.[9] AAV5-*GUCY2D* and AAV5-*Gucy2e* vectors were made at Sanofi via TTx using the same input plasmids and protocol as described previously.[10] Generation of AAV vectors by the PCL method was performed at Sanofi. In brief, a HeLa-based PCL was created after transfection of HeLaS3 cells (ATCC CCL-2.2) with a single plasmid containing the following elements: AAV2 rep genes and the cap5 gene, the *GUCY2D* vector genome flanked by AAV2 ITRs, and a puromycin resistance gene. Transfected cells were grown in the presence of puromycin to isolate stable integrants, which were subsequently screened for AAV productivity after infection with wild-type (WT) Ad5 virus.[21,22] Purification of AAV from both production platforms was achieved using a 2 CC method and titered using TaqMan qPCR targeting the bGH poly(A) region.[10] Vector genomes were also quantified in dose retains via qPCR using the same primer/probe set. All dose retains were run on the same assay plate. The primer/probe sequences are as follows: forward, 5′-TCTAGTTGCCAGCCATCTG TTGT-3′; reverse, 5′-TGGGAGTGGCACCTTCCA-3′; probe, 5′-6F AM-TCCCCCGTGCCTTCCTTGACC-TAMRA-3′. Copy numbers were estimated by comparison with a standard curve generated with a plasmid that contained bGH poly(A) target sequences.

Sample preparation for AUC

Purified vector, at a concentration of 2.0×10^{12}–5.0×10^{12} vg/mL, was buffer exchanged into phosphate-buffered saline (PBS), pH 7.2, using a 10,000 MWCO Slide-a-Lyzer (Thermo Scientific, Waltham, MA). The AAV vector absorbance signal was determined by optical density 260 (OD_{260}) using spectrophotometric methods. For consistency, the samples were adjusted to a target concentration (OD_{260} of between 0.2 and 0.8) by direct dilution with PBS or further concentrated using an Amicon Ultra-0.5/30K MWCO Centrifugal Filter Device (Merck, Darmstadt, Germany).

Sedimentation velocity AUC data acquisition

Sedimentation velocity AUC analysis was performed using a Proteome Lab XL-I (Beckman Coulter, Indianapolis, IN). Four hundred microliters of sample was loaded into the sample sector of a two-sector velocity cell, and 400 μL of PBS was loaded into the corresponding reference sector. The sample was placed in the four-hole rotor and allowed to equilibrate in the instrument until a temperature of 20°C and a full vacuum were maintained for 1 h. Sedimentation velocity centrifugation was performed at 20,000 rpm and 20°C. Absorbance (260 nm) and Raleigh interference optics were used to simultaneously record the radial concentration as a function of time until the lightest sedimenting component cleared the optical window (1.2 h).[11]

AUC data analysis

The percentage of virions containing a full genome was determined by analyzing approximately 60 scans using the absorbance detection method and the SEDFIT continuous-size C(S) distribution model as described in Burnham et al.[11] The results of the AUC analyses are plotted as the normalized differential coefficient distribution value, C(S), versus the sedimentation coefficient (S).

Absorbance optics 260 nm

Absorbance data require use of extinction coefficients to calculate the molar concentration and the percent value of the empty and

genome-containing capsids. Molar concentrations of genome-containing and empty capsids were calculated using Beer's law, and the percentages of full genome-containing and empty capsids were calculated. The relative percentage of each peak in the C(S) distribution is calculated based on the molar concentration of each species in relation to the sum of the molar concentration of all species in the distribution. The molar extinction coefficient (e) for the AAV DNA-containing capsid was determined using the formula $\varepsilon_{260/DNA} + \varepsilon_{260/AAV\ capsid}$, as described by Burnham et al.[11] The relative percentage of each peak in the C(S) distribution is calculated based on the molar concentration of each species in relation to the sum of the molar concentration of all species in the distribution. The molar concentration of the genome-containing vector and the empty virion was calculated using Beer's law, and the fractional content of each capsid species was reported as a percentage of the total.[11]

Comparison of AAV5-based capsid mutants *in vitro*

Site-directed mutational analyses of surface-exposed tyrosine residues on AAV5 capsid proteins were generated using the published AAV5 road map.[24] Site-directed mutagenesis of Y263, Y719, and Y436 were performed by changing tyrosine residues to phenylalanine residues (Y-F). AAV5 (Y263+719F) and AAV5(Y436+719F) capsid mutants were generated and AAV5(Y263+719F)- and AAV5(Y436+719F)-mCherry vectors were generated for analysis *in vitro*. Those residues were chosen because they were predicted to be surface exposed based on the relative position on the homologous AAV2 capsid. ARPE-19 cells (ATCC), seeded at a density of 1e4 cells/well in a 96-well plate, were infected with AAV5-based vectors containing a self-complementary smCBA-mCherry genome at an MOI of 2,000 or 10,000. Three days p.i., cells were collected and subjected to flow cytometry to quantify reporter (mCherry) fluorescence. mCherry expression was measured by multiplying the mean mCherry fluorescence by the number of positive cells, as described previously.[25,26] Transduction assays were conducted in triplicate.

Animal ethics statement

GC1KO[27] and GCDKO mice[5] were bred and maintained at the University of Florida Health Science Center Animal Care Services Facility under a 12-h/12-h light/dark cycle. Food and water were available *ad libitum*. All experiments were approved by the University of Florida's Institutional Animal Care and Use Committee and were conducted in accordance with the Association for Research in Vision and Ophthalmology's (ARVO's) Statement for the Use of Animals in Ophthalmic and Vision Research and with National Institutes of Health regulations.

Non-GLP AAV5-GFP pharmacology studies and GLP tox studies using cynomolgus monkeys (*Macaca fascicularis*) were performed at Covance (Madison, WI), the drug development business of Laboratory Corporation of America Holdings (LabCorp, Burlington, NC), and the latter were conducted in compliance with GLP for nonclinical laboratory studies requirements. Covance Laboratories is fully accredited by the Association for Assessment and Accreditation of Laboratory Animal Care (AAALAC). All procedures in the protocol complied with applicable animal welfare acts and were approved by the local institutional animal care and use committee (IACUC).

Subretinal injections in mice

One microliter of vector was delivered subretinally to GC1KO or GCDKO mice between P21 and P35. Identification of the vector and the respective doses used in each experiment are outlined in Tables 1 and 2 and in the supplemental information. All injections were performed under a Leica M80 stereomicroscope according to methods published previously.[28] Injection blebs were imaged immediately after injection, and further analysis was carried out only on animals that received comparable successful injections ($\geq$60% retinal detachment and minimal complications). These exclusion criteria explain the difference between the number of animals dosed (which appears in Tables 1 and 2) versus the number of animals that were used for statistical comparisons in the various *in vivo* studies (which appear in the associated figures).

Quantification of AAV-mediated GFP expression in the mouse retina

Four weeks after subretinal injection of AAV5-based vectors in GCDKO mice, GFP fluorescence was documented in life using a Micron III fundoscope (Phoenix Research Laboratories) with a green fluorescence filter. Image exposure settings remained consistent across all mice.

Analysis of retinal function in mice via electroretinogram

Rod-mediated (scotopic) and cone-mediated (photopic) ERG recordings were performed on GC1KO and GCDKO mice beginning 1 month p.i. Measurements continued at monthly intervals for as long as 3 months p.i. (experimental timelines are detailed under Results). The first three mouse studies detailed under Results incorporated the UTAS Visual Diagnostic System equipped with Big Shot Ganzfeld (LKC Technologies, Gaithersburg, MD). After overnight dark adaptation, scotopic (rod-mediated) ERGs were elicited at intensities ranging from −20 to 0 dB with interstimulus intervals of 30 s, averaged from five measurements at each intensity. Mice were then light adapted to a 30 cd-s/m^2 white background for 5 min. Photopic (cone-mediated) responses were elicited with intensities ranging from −3 to 10 dB. Fifty responses with interstimulus intervals of 0.4 s were recorded in the presence of a 20 cd-s/m^2 white background and averaged at each intensity. The b wave amplitudes were defined as the difference between the a wave troughs to the positive peaks of each waveform. At each time point, maximum scotopic and photopic b wave amplitudes (those generated at 0 dB and 10 dB, respectively) from all injected and uninjected (contralateral) eyes were averaged as mean ± standard deviation. For photopic recordings, rods were photobleached prior to initiation of stimuli associated with ERG recordings. An animal was defined as a responder when an apparent waveform existed and photopic and scotopic b wave responses were greater than 15 and 50 μV, respectively.

ERG recordings in the last three mouse studies detailed under Results were obtained using a fully integrated Celeris system (Diagnosys,

Lowell MA). After overnight dark adaptation, scotopic (rod-mediated) ERGs were elicited at intensities ranging from 0.025–2.5 cd-s/m^2 with intervals of 6 s between each stimulus intensity and 5 s between each sweep/measurement of the same intensity, averaged from five sweeps per eye. Mice were then light-adapted to a 30 cds/m^2 white background for 5 min. Photopic (cone-mediated) responses were elicited with intensities ranging from 1.25–25 cd-s/m^2. Fifty responses with intervals of 6 s between each stimulus intensity and 0.4 s between each sweep of the same intensity were recorded in the presence of a 30 cds/m^2 white background and averaged at each intensity. The b wave amplitudes were defined as the difference between the a wave troughs to the positive peaks of each waveform. The maximum scotopic b wave amplitudes elicited from the 0.25 cd-s/m^2 stimulus were recorded and averaged as mean ± standard deviation. Irrespective of photopic stimulus, the maximum photopic b wave response amplitudes from all treated and uninjected eyes were averaged as mean ± standard deviation. After our shift to this much more sensitive ERG machine (which can detect aptitude improvements in the single digits), responders were defined as those that had an apparent waveform with careful deference to destructive or constructive interference/baseline drift.

Statistical comparisons between treated eyes versus uninjected controls were conducted using multiple paired t tests with Holm-Sidak correction for multiple comparisons. Statistical comparisons across treatment groups were conducted using one-way ANOVA with Tukey's post-test. Statistical comparisons across multiple treatment groups and multiple time points were conducted with two-way ANOVA with Sidak's post-test. In all experiments, responses from all injected eyes were averaged.

Analysis of retinal structure in mice via OCT

OCT analysis was performed on GC1KO and GCDKO mice 1 month p.i. and continued monthly for as long as 3 months p.i. (Results). Briefly, scans were collected noninvasively using the Bioptigen system (Durham, NC). ONL thickness was manually calculated. Three lateral images (nasal to temporal) were collected: (1) 3 mm above the meridian crossing through the optic nerve head (ONH), (2) the meridian passing through the ONH, and (3) 3 mm below the ONH meridian. Three points were placed on identical locations on each meridian across samples. ONL thickness was measured at each point, and values were compared with a two-way ANOVA with Tukey's post-test, with $p < 0.05$ considered significant.

Analysis of visually guided behavior in mice via OptoMotry

Behavioral analysis was conducted in the study comparing therapeutic response to the AAV containing the murine *Gucy2e* versus human *GUCY2D* coding sequence. GC1KO with representative cone-mediated ERG response amplitudes in treated eyes were selected for testing. This included mice from group 1 (n = 2, at approximately 12 weeks p.i.), group 2 (n = 2, at approximately 15 weeks p.i.), group 3 (n = 3, at approximately 15 weeks p.i.), group 4 (n = 2, at approximately 10 weeks p.i.), group 5 (n = 3, at approximately 20 weeks p.i.), and group 6 (n = 6, at approximately 13 and 20 weeks p.i.). Testing was also performed on three C57BL6 WT mice at approximately 8 weeks of age to serve as positive controls.

Briefly, a virtual reality chamber was created with four computer monitors facing into a square (17-in monitors were used with mice). A virtual cylinder, covered with a vertical sine-wave grating, was projected onto the monitors using software (OptoMotry, CerebralMechanics). The animal was placed on a platform in the center of the square, and a video camera, situated above the animal, provided real-time video feedback on another computer screen. Mice were allowed to move freely on the platform, and the spatial frequency of the grating was "clamped" as the animals viewing position by manually tracking the head and repeatedly recentering the cylinderon the head as the mouse moved. A trial began when the experimenter centered the virtual drum on the head; a drifting (12°/s) grating then appeared. The experimenter judged whether the mouse made slow tracking movements with its head to follow the drifting grating. Large repositioning and grooming movements were ignored, and the trial was restarted when the presence or absence of tracking was not clear. Visual thresholds were obtained with a staircase procedure in which the step size was halved after each reversal and was terminated when the step size became smaller than the hardware resolution (0.003 c/d, 0.2% contrast). One staircase was done for each direction of rotation of the optokinetic stimulus, with the two staircases being interleaved. This facilitated measurements of visually guided behavior from the right (treated) and left (untreated) eyes. To avoid the possibility of experimenter bias affecting the results, at least two experimenters were involved in all behavior tests. Both experimenters had to agree that tracking was observed before selecting "yes" and moving to the next spatial frequency. The maximum spatial frequency capable of driving head tracking was determined and recorded for each animal, and the average thresholds and standard deviations from each cohort were graphed.

Quantification of AAV5-hGRK1-mediated GFP expression in subretinally injected macaques

Animals (males and females) used for evaluation of AAV5-hGRK1-GFP were between 30 and 53 months old, and their body weights ranged from 2–5 kg. Using methods published previously,[29] both eyes of each cynomolgus macaque received a single 120-μL subretinal injection directed under the fovea. The study was separated into 6 groups with multiple animals per group, in which both eyes were injected with AAV5-hGRK1-GFP at 1.0×10^{10}, 3.3×10^{10}, 1.0×10^{11}, 3.3×10^{11}, 6.7×10^{11}, or 1.0×10^{12} vg/mL (Table S11). Fundus ocular photography was conducted after dosing on day 1, and fundus autofluorescence images were captured once prior to injection and during weeks 4 and 6 of the study. All animals were terminated 6 weeks after injection, and eyes were collected and embedded in paraffin for immunofluorescence analysis. Eyes were sectioned onto slides and stained for GFP, DAPI, and proteins expressed exclusively in PRs to aid identification of PRs. Six slides from each eye were generated: one slide inferior to the fovea, four slides immediately adjacent/through the fovea, and one slide superior to the fovea. The slide set from each eye was reviewed, and three slides were selected for

analysis: one slide inferior to the fovea, one through the center of the fovea, and one superior to the fovea (Figure S3A). The PR layer was imaged from one border of the subretinal bleb to the other (an example is shown in Figure S3B). Morphometric analysis was performed using NIH ImageJ (v.1.49t) to determine the percentage of PRs expressing the GFP transgene within the borders of the subretinal bleb. Images spanning the subretinal bleb consisted of two 16-bit TIFF images obtained at exactly the same specimen position with a fluorescein isothiocyanate (FITC) or DAPI filter cube. When GFP was not observed, an image set was not collected. When GFP was observed, 7–23 image sets were collected. Each image was opened with ImageJ, and each image's color was converted to RGB. Contrast was enhanced in the green channel of the FITC image. The color balance command was used to move the "minimum" slider to the start of the histogram, the "maximum slider" to the end of the histogram, and the "brightness" slider to eliminate background fluorescence. The surface area of the ONL was measured by selecting the ONL, using the "Measure" command to measure the surface area (square pixels), and the result (PR_{total}) was recorded. A mask of the ONL was created by using the "Make Inverse" command to select everything except the ONL in the DAPI image, replacing all colors in this selection with black, and copying the mask onto the clipboard. The mask was applied to the FITC image to reveal only the PRs. Thresholding was applied to the FITC image with the "Color Threshold" command (color space was set to "HSB," the threshold method was set to "Default," and the "Brightness" slider was moved until all the green pixels were selected). The surface area of the pixels was measured with the "Analyze Particles" tool (size was set to 0-Infinity, circularity was set to 0.00–1.00, with "Summarize" radio box checked) and the result ($PR_{transduced}$) was recorded. The percentage of transduced PRs was determined using the following formula: percentage of transduced PRs = $PR_{transduced}/PR_{total} \times 100$. As an example of the analysis of immunofluorescence, the percentage of PRs expressing GFP after subretinal administration of AAV5-hGRK1-EGFP at 4.0×10^{10} vg/eye is shown in Figure S3C. Each bar in the graph represents the percentage of PRs expressing GFP from the field of view of one microscope image. The images were sequentially collected from one edge of the subretinal bleb to the other. Each bar represents the percentage of GFP-expressing PRs in one microscope image of the subretinal bleb. The total percentage for each bleb is presented, as well as the dose group average ± standard deviation. The microscope images that contained the fovea were marked with "f" on the corresponding bar or bars.

Rat BD study

Long Evans rats were received from Charles River Laboratories (Kingston, NY, USA). The animals were approximately 9 weeks old and weighed between 256 and 359 g (males) and 184 and 248 g (females) at initiation of dosing. Unilateral subretinal injections at a dose volume of 2 μL/right eye/animal were performed, with left eyes serving as untreated controls. A topical antibiotic (tobramycin) was applied to both eyes twice on the day before and after each injection. During dosing, animals were maintained under anesthesia with isoflurane/oxygen gas. The conjunctivae were flushed with sterile saline. Mydriatic and topical anesthetic drops were applied to the right eye as needed. A 32G needle connected to a Hamilton syringe was used to administer the test and reference items to the subretinal space. Subretinal injections were performed using an operating microscope by a board-certified veterinary ophthalmologist. Both eyes were examined by slit-lamp biomicroscopy and/or indirect ophthalmoscopy after completion of each treatment to confirm the dose location, appearance, presence or absence of a bleb, and quadrant in which the bleb was located and to document any abnormalities (vitreous and retina) caused by the administration procedure.

Mortality/moribundity checks were performed twice daily, cageside observations were performed daily, detailed examinations and individual body weight measurements were performed weekly, and food consumption was measured weekly. Ophthalmology examinations were conducted by a board-certified ophthalmologist once before treatment, again on day 3 (all animals), and then prior to necropsy during week 2, week 4, and month 3 on surviving animals. All animals were subjected to funduscopic (indirect ophthalmoscopy) and biomicroscopic (slit lamp) examinations.

Animals surviving until scheduled euthanasia (day 4, day 15, day 29, and day 92) underwent exsanguination from the abdominal aorta after isoflurane anesthesia and blood sample collection from the abdominal aorta. A target volume of 2 mL of blood was collected. Group 1 animals were euthanized first, followed by group 2 and then group 3, in a manner to minimize risk of tissue contamination. Quantitation of vector DNA was performed for all groups in 13 tissues/fluids (Tables S17 and S18), assessed by qPCR. The vector copy numbers were determined using a PCR-based titer assay. For the tissues that tested positive for vector DNA, RNA was isolated to test for the presence of *GUCY2D* transgene expression by qRT-PCR analysis (excluding eyes and optic nerves).

NHP tox study designs

Pre-screening was performed to determine levels of AAV5 neutralizing antibodies (NAb), and animals with titers of 1:8 or less were assigned to the study. Animals were 2–3 years old, and their body weights ranged from 2.1–3.4 kg for males and 2.2–3.0 kg for females. Using methods published previously,[29] cynomolgus macaques received submacular subretinal injections of AAV-hGRK1-*GUCY2D* in their right eyes at a dose volume of 150 μL. The vector concentrations used in both GLP tox studies are summarized in Tables 1 and 2. Steroid prophylaxis was employed only in GLP tox study 2 (see Table 2 for details).

Health monitoring was performed twice daily, qualitative food consumption was measured once daily, and detailed clinical observations were conducted at least once during the predose phase and for each animal prior to dosing on day 1 and weekly throughout the dosing phase. All abnormal findings were recorded. OEs were performed using slit-lamp biomicroscopy, indirect ophthalmoscopy, and measurement of IOP. In tox study 1, OEs were conducted at least once during the predose phase (at least 1 week after aqueous tap collection); on

days 8 and 15, once between days 20 and 25 (cohorts 3 and 4); on days 29, 43, and 58/59 (cohorts 1 and 2) of the dosing phase (during weeks 2, 3, 4/5, 7, and 9, respectively); and during weeks 11, 13, 17, 21, 26, 30, 34, and 39 of the dosing phase. On day 18 of the dosing phase (cohort 4), OEss were conducted for animals in group 5, cohort 4 to monitor ophthalmic findings and treatment. In tox study 2, OEs were conducted once during the predose phase for all animals and on days 8, 16, 22, 29, 36, 43, 50, 57, 64, 71, 78, 85, and 92 of the dosing phase. Aqueous cells and flare and vitreous cells were scored as described previously.[30] Aqueous and vitreous cell scores were assigned using an estimate of cells per single 0.2-mm field of the focused slit-lamp beam as 0 (no cells), trace (1–5 cells), 1+ (5–25 cells), 2+ (25–50 cells), 3+ (50–100 cells), or 4+ (>100 cells). Aqueous flare was scored, on the basis of the presence of protein in the anterior chamber, as 0 (no visible protein), trace (visible only to an experienced observer using a small, bright focal light source and magnification), 1+ (mild), 2+ (moderate), 3+ (moderate but more than 2+), or 4+ (severe). Vitreous haze was scored according to the Standardization of Uveitis Nomenclature (SUN) method.[31]

In tox study 1, ffERGs were done once during the predose phase and during weeks 11, 24, and 37 of the dosing phase for all surviving animals. Multi-focal ERGs were done once during the predose phase and during weeks 4, 12, 25, and 38 of the dosing phase for all surviving animals. Scotopic tests were done using stimuli as follows: a dim short wavelength (scotopic 34-dB blue single flash), along wavelength (scotopic 8-dB red single flash), a mixed rod-cone stimulus (scotopic 0-dB white single flash), and oscillatory potentials (high-frequency components digitally filtered from the scotopic 0-dB white single flash condition). For multi-focal ERG, the stimulus was an unstretched 103 hexagonal array using a 13.3-ms base rate. The grid was composed of bright (approximate 200 cd/m^2 white light) and dark (approximate 1 cd/m^2 white light) patches. Spectral domain OCT (sdOCT) was conducted on both eyes once during the predose phase and on the right eye only during weeks 2, 5, 9, 13, 17/18, 21, 26, 30, 34, and 39 of the dosing phase.

In tox study 2, ffERG was conducted once during the predose phase and once during weeks 4 and 12 of the dosing phase. Scotopic ffERG tests were done using identical methods as described above. Photopic tests were also done using stimuli as follows: single white flashes (photopic 0-dB single flash) and flashes delivered at a rate of 30.3 Hz (photopic 0-dB, 30.3-Hz white). Visually evoked potential tests were done using monocular stimulation (with the unstimulated eye occluded with an opaque patch); recordings were made unilaterally through each eye. An average of 80 flashes with an interstimulus interval of 0.244 s (4.1 Hz) was used. mfERG was conducted once during the predose phase and once during weeks 4 and 12 of the dosing phase as described above. sdOCT was conducted once during the predose phase and once during weeks 5 and 13 of the dosing phase.

Blood samples were collected to determine BD of the test article, expression of the transgene, cellular immune response, and immunogenicity. Aqueous humor was collected to determine immunogenicity. In tox study 1, blood samples (approximately 2.0 mL) were collected via the femoral vein at least twice during the predose phase and once during weeks 2, 5, 9, 13, 17, 21, 26, 30, 34, and 39 of the dosing phase from all animals. Aqueous humor samples (approximately 50 μL) were collected from both eyes at least once during the predose phase and on the day of scheduled sacrifice at necropsy. In tox study 2, blood samples were collected twice during the predose phase and once during weeks 5 and 13 of the dosing phase. Total DNA was extracted from all sample types designated for qPCR analysis, and the AAV5 vector DNA concentration (vector genomes per milligram of host DNA) was determined using a validated qPCR method. Analysis of blood samples from each animal continued until two consecutive negative postdose qPCR results were obtained. RNA was extracted from blood samples designated for qRT-PCR analysis. Pending positive qPCR results, transgene mRNA concentration was determined from samples collected at the same interval using a validated qRT-PCR method. Serum and aqueous humor were analyzed for anti-AAV5 antibodies and antibodies to the transgene product using ELISA. Cellular immune responses to the capsid and transgene were also analyzed in tox study 1. Peripheral blood mononuclear cells (PBMCs) were tested for the production of interferon γ (IFN-γ) when exposed to AAV5 and transgene peptide libraries by an ELISpot assay under non-GLP conditions.

Clinical laboratory procedures were similar in both tox studies. In tox study 1, blood samples designated for clinical pathology (hematology/coagulation/clinical chemistry) were collected twice during the predose phase and during weeks 2, 5, 9, 13, 17, 21, 26, 30, 34, and 39 of the dosing phase. Urine samples were also collected for urinalysis and urine chemistry once during the predose phase and during weeks 2, 5, 9, 13, 17, 21, 26, 30, 34, and 39 of the dosing phase. In tox study 2, blood samples for clinical pathology were collected twice during the predose phase, once during week 7, and on day 92.

In tox study 1, the following tissues were collected from all animals scheduled for an interim sacrifice: eye (right), optic nerve (right), occipital lobe (right and left), spleen, lesions, liver. From right eyes, two 6-mm diameter punches were collected (one within the bleb area, another outside of the bleb). The remaining posterior segment was also collected for a total of three samples/eye, all of which were designated for qPCR analysis. For remaining tissues, two samples, of ~5 × 5 × 5 mm each were collected (one for qPCR and one for qRT-PCR analysis). Tissues determined by qPCR analysis to be positive were subject to qRT-PCR analysis.

Terminal body weights were recorded for sacrificed animals. Macroscopic examination of external features; external orifices; abdominal, thoracic, and cranial cavities; organs; and tissues was performed at necropsy. Tissues from each animal were preserved in 10% formalin, embedded in paraffin, and sectioned, and slides were prepared with hematoxylin and eosin and reviewed by a pathologist. Tox study 1 analyzed a very comprehensive set of organs/tissues, whereas tox study 2 analysis was restricted to eyes only.

DATA AVAILABILITY

Materials and protocols will be distributed to qualified scientific researchers for non-commercial, academic purposes.

SUPPLEMENTAL INFORMATION

Supplemental information can be found online at https://doi.org/10.1016/j.omtm.2022.12.007.

ACKNOWLEDGMENTS

This work was sponsored by Sanofi. S.E.B is a founder, director, and consultant for Atsena Therapeutics. S.L.B. is a founder and consultant for Atsena Therapeutics. S.E.B. and S.L.B. are inventors of a patent related to this technology. A.S., C.O., M.L., J.M., R.B., D.C., and A.M.-W. were employees of Sanofi when this work was conducted. D.E. is an employee of Atsena Therapeutics.

AUTHOR CONTRIBUTIONS

S.E.B., S.L.B., A.M.-W., A.S., C.O., J.M., M.L., and D.C. conceived and directed the study. S.E.B., S.L.B., A.S., A.M.-W., C.O., J.M., M.L., and D.C. reviewed, analyzed, and interpreted the data. J.J.P., D.F. and K.T.M. collected the data. R.B. collated data. S.E.B and S.L.B. wrote the manuscript. D.M.E. assisted with figure preparation.

DECLARATION OF INTERESTS

S.E.B. and S.L.B. are cofounders of Atsena Therapeutics, a company with related interests. They are recipients of research funding from Atsena Therapeutics.

REFERENCES

1. Jacobson, S.G., Cideciyan, A.V., Peshenko, I.V., Sumaroka, A., Olshevskaya, E.V., Cao, L., Schwartz, S.B., Roman, A.J., Olivares, M.B., Sadigh, S., et al. (2013). Determining consequences of retinal membrane guanylyl cyclase (RetGC1) deficiency in human Leber congenital amaurosis en route to therapy: residual cone-photoreceptor vision correlates with biochemical properties of the mutants. Hum. Mol. Genet. *22*, 168–183. https://doi.org/10.1093/hmg/dds421.

2. Bouzia, Z., Georgiou, M., Hull, S., Robson, A.G., Fujinami, K., Rotsos, T., Pontikos, N., Arno, G., Webster, A.R., Hardcastle, A.J., et al. (2020). GUCY2D-Associated leber congenital amaurosis: a retrospective natural history study in preparation for trials of novel therapies. Am. J. Ophthalmol. *210*, 59–70. https://doi.org/10.1016/j.ajo.2019.10.019.

3. Aguirre, G.K., Butt, O.H., Datta, R., Roman, A.J., Sumaroka, A., Schwartz, S.B., Cideciyan, A.V., and Jacobson, S.G. (2017). Postretinal structure and function in severe congenital photoreceptor blindness caused by mutations in the GUCY2D gene. Invest. Ophthalmol. Vis. Sci. *58*, 959–973. https://doi.org/10.1167/iovs.16-20413.

4. Jacobson, S.G., Cideciyan, A.V., Ho, A.C., Peshenko, I.V., Garafalo, A.V., Roman, A.J., Sumaroka, A., Wu, V., Krishnan, A.K., Sheplock, R., et al. (2021). Safety and improved efficacy signals following gene therapy in childhood blindness caused by GUCY2D mutations. iScience *24*, 102409. https://doi.org/10.1016/j.isci.2021.102409.

5. Baehr, W., Karan, S., Maeda, T., Luo, D.G., Li, S., Bronson, J.D., Watt, C.B., Yau, K.W., Frederick, J.M., and Palczewski, K. (25/2007 2007). The function of guanylate cyclase 1 (GC1) and guanylate cyclase 2 (GC2) in rod and cone photoreceptors. J. Biol. Chem. *282*, 8837–8847.

6. Boye, S.L., Peshenko, I.V., Huang, W.C., Min, S.H., McDoom, I., Kay, C.N., Liu, X., Dyka, F.M., Foster, T.C., Umino, Y., et al. (2013). AAV-mediated gene therapy in the guanylate cyclase (RetGC1/RetGC2) double knockout mouse model of Leber congenital amaurosis. Hum. Gene Ther. *24*, 189–202. https://doi.org/10.1089/hum.2012.193.

7. Petrs-Silva, H., Dinculescu, A., Li, Q., Min, S.H., Chiodo, V., Pang, J.J., Zhong, L., Zolotukhin, S., Srivastava, A., Lewin, A.S., and Hauswirth, W.W. (2009). High-efficiency transduction of the mouse retina by tyrosine-mutant AAV serotype vectors. Mol. Ther. *17*, 463–471. https://doi.org/10.1038/mt.2008.

8. Boye, S.E., Boye, S.L., Pang, J., Ryals, R., Everhart, D., Umino, Y., Neeley, A.W., Besharse, J., Barlow, R., and Hauswirth, W.W. (2010). Functional and behavioral restoration of vision by gene therapy in the guanylate cyclase-1 (GC1) knockout mouse. PLoS One *5*, e11306. https://doi.org/10.1371/journal.pone.0011306.

9. Zolotukhin, S., Potter, M., Zolotukhin, I., Sakai, Y., Loiler, S., Fraites, T.J., Jr., Chiodo, V.A., Phillipsberg, T., Muzyczka, N., Hauswirth, W.W., et al. (2002). Production and purification of serotype 1, 2, and 5 recombinant adeno-associated viral vectors. Methods *28*, 158–167.

10. Nass, S.A., Mattingly, M.A., Woodcock, D.A., Burnham, B.L., Ardinger, J.A., Osmond, S.E., Frederick, A.M., Scaria, A., Cheng, S.H., and O'Riordan, C.R. (2018). Universal method for the purification of recombinant AAV vectors of differing serotypes. Mol. Ther. Methods Clin. Dev. *9*, 33–46. https://doi.org/10.1016/j.omtm.2017.12.004.

11. Burnham, B., Nass, S., Kong, E., Mattingly, M., Woodcock, D., Song, A., Wadsworth, S., Cheng, S.H., Scaria, A., and O'Riordan, C.R. (2015). Analytical ultracentrifugation as an approach to characterize recombinant adeno-associated viral vectors. Hum. Gene Ther. Methods *26*, 228–242. https://doi.org/10.1089/hgtb.2015.048.

12. Qi, Y., Dai, X., Zhang, H., He, Y., Zhang, Y., Han, J., Zhu, P., Zhang, Y., Zheng, Q., Li, X., et al. (2015). Trans-corneal subretinal injection in mice and its effect on the function and morphology of the retina. PLoS One *10*, e0136523. https://doi.org/10.1371/journal.pone.0136523.

13. Boye, S.E., Alexander, J.J., Boye, S.L., Witherspoon, C.D., Sandefer, K.J., Conlon, T.J., Erger, K., Sun, J., Ryals, R., Chiodo, V.A., et al. (2012). The human rhodopsin kinase promoter in an AAV5 vector confers rod- and cone-specific expression in the primate retina. Hum. Gene Ther. *23*, 1101–1115. https://doi.org/10.1089/hum.2012.125.

14. Jacobson, S.G., Acland, G.M., Aguirre, G.D., Aleman, T.S., Schwartz, S.B., Cideciyan, A.V., Zeiss, C.J., Komaromy, A.M., Kaushal, S., Roman, A.J., et al. (2006). Safety of recombinant adeno-associated virus type 2-RPE65 vector delivered by ocular subretinal injection. Mol. Ther. *13*, 1074–1084.

15. Jacobson, S.G., Boye, S.L., Aleman, T.S., Conlon, T.J., Zeiss, C.J., Roman, A.J., Cideciyan, A.V., Schwartz, S.B., Komaromy, A.M., Doobrajh, M., et al. (2006). Safety in nonhuman primates of ocular AAV2-RPE65, a candidate treatment for blindness in Leber congenital amaurosis. Hum. Gene Ther. *17*, 845–858.

16. Roman, A.J., Boye, S.L., Aleman, T.S., Pang, J.J., McDowell, J.H., Boye, S.E., Cideciyan, A.V., Jacobson, S.G., and Hauswirth, W.W. (2007). Electroretinographic analyses of Rpe65-mutant rd12 mice: developing an in vivo bioassay for human gene therapy trials of Leber congenital amaurosis. Mol. Vis. *13*, 1701–1710.

17. https://www.fda.gov/media/109906/download.

18. Rodríguez-Bocanegra, E., Wozar, F., Seitz, I.P., Reichel, F.F.L., Ochakovski, A., Bucher, K., Wilhelm, B., Bartz-Schmidt, K.U., Peters, T., and Fischer, M.D.; RD-CURE Consortium (2021). Longitudinal evaluation of hyper-reflective foci in the retina following subretinal delivery of adeno-associated virus in non-human primates. Transl. Vis. Sci. Technol. *10*, 15. https://doi.org/10.1167/tvst.10.6.15.

19. Reichel, F.F., Dauletbekov, D.L., Klein, R., Peters, T., Ochakovski, G.A., Seitz, I.P., Wilhelm, B., Ueffing, M., Biel, M., Wissinger, B., et al. (2017). AAV8 can induce innate and adaptive immune response in the primate eye. Mol. Ther. *25*, 2648–2660. https://doi.org/10.1016/j.ymthe.2017.08.018.

20. Boye, S.L., Conlon, T., Erger, K., Ryals, R., Neeley, A., Cossette, T., Pang, J., Dyka, F.M., Hauswirth, W.W., and Boye, S.E. (2011). Long-term preservation of cone photoreceptors and restoration of cone function by gene therapy in the guanylate cyclase-1 knockout (GC1KO) mouse. Invest. Ophthalmol. Vis. Sci. *52*, 7098–7108. https://doi.org/10.1167/iovs.11-7867.

21. Martin, J., Frederick, A., Luo, Y., Jackson, R., Joubert, M., Sol, B., Poulin, F., Pastor, E., Armentano, D., Wadsworth, S., and Vincent, K. (2013). Generation and characterization of adeno-associated virus producer cell lines for research and preclinical vector production. Hum. Gene Ther. Methods *24*, 253–269. https://doi.org/10.1089/hgtb.2013.046.

22. Thorne, B.A., Takeya, R.K., and Peluso, R.W. (2009). Manufacturing recombinant adeno-associated viral vectors from producer cell clones. Hum. Gene Ther. *20*, 707–714. https://doi.org/10.1089/hum.2009.070.

23. Boye, S.L., Peterson, J.J., Choudhury, S., Min, S.H., Ruan, Q., McCullough, K.T., Zhang, Z., Olshevskaya, E.V., Peshenko, I.V., Hauswirth, W.W., et al. (2015). Gene Therapy Fully Restores Vision to the All-Cone Nrl(-/-) Gucy2e(-/-) Mouse Model of Leber Congenital Amaurosis-1. Hum. Gene Ther. *26*, 575–592. https://doi.org/10.1089/hum.2015.053.

24. Govindasamy, L., DiMattia, M.A., Gurda, B.L., Halder, S., McKenna, R., Chiorini, J.A., Muzyczka, N., Zolotukhin, S., and Agbandje-McKenna, M. (2013). Structural insights into adeno-associated virus serotype 5. J. Virol. *87*, 11187–11199. https://doi.org/10.1128/JVI.00867-13.

25. Boye, S.L., Bennett, A., Scalabrino, M.L., McCullough, K.T., Van Vliet, K., Choudhury, S., Ruan, Q., Peterson, J., Agbandje-McKenna, M., and Boye, S.E. (2016). Impact of heparan sulfate binding on transduction of retina by recombinant adeno-associated virus vectors. J. Virol. *90*, 4215–4231. https://doi.org/10.1128/JVI.00200-16.

26. Ryals, R.C., Boye, S.L., Dinculescu, A., Hauswirth, W.W., and Boye, S.E. (2011). Quantifying transduction efficiencies of unmodified and tyrosine capsid mutant AAV vectors in vitro using two ocular cell lines. Mol. Vis. *17*, 1090–1102.

27. Yang, R.B., Robinson, S.W., Xiong, W.H., Yau, K.W., Birch, D.G., and Garbers, D.L. (1999). Disruption of a retinal guanylyl cyclase gene leads to cone-specific dystrophy and paradoxical rod behavior. J. Neurosci. *19*, 5889–5897.

28. Boye, S.L., Choudhury, S., Crosson, S., Di Pasquale, G., Afione, S., Mellen, R., Makal, V., Calabro, K.R., Fajardo, D., Peterson, J., et al. (2020). Novel AAV44.9-based vectors display exceptional characteristics for retinal gene therapy. Mol. Ther. *28*, 1464–1478. https://doi.org/10.1016/j.ymthe.2020.04.002.

29. Nork, T.M., Murphy, C.J., Kim, C.B.Y., Ver Hoeve, J.N., Rasmussen, C.A., Miller, P.E., Wabers, H.D., Neider, M.W., Dubielzig, R.R., McCulloh, R.J., and Christian, B.J. (2012). Functional and anatomic consequences of subretinal dosing in the cynomolgus macaque. Arch. Ophthalmol. *130*, 65–75. https://doi.org/10.1001/archophthalmol.2011.295.

30. Martin, P.L., Miller, P.E., Mata, M., and Christian, B.J. (2009). Ocular inflammation in cynomolgus macaques following intravenous administration of a human monoclonal antibody. Int. J. Toxicol. *28*, 5–16. https://doi.org/10.1177/1091581809333987.

31. Jabs, D.A., Nussenblatt, R.B., and Rosenbaum, J.T.; Standardization of Uveitis Nomenclature SUN Working Group (2005). Results of the first international workshop. Am. J. Ophthalmol. *140*, 509–516. https://doi.org/10.1016/j.ajo.2005.03.057.

OMTM, Volume *28*

Supplemental information

Preclinical studies in support of phase I/II clinical trials to treat *GUCY2D*-associated Leber congenital amaurosis

Sanford L. Boye, Catherine O'Riordan, James Morris, Michael Lukason, David Compton, Rena Baek, Dana M. Elmore, James.J. Peterson, Diego Fajardo, K. Tyler McCullough, Abraham Scaria, Alison McVie-Wylie, and Shannon E. Boye

Supplemental Text

Detailed Description of Findings in NHP GLP Tox Study #1.

Clinical ophthalmic examination noted the subretinal injection site, when visible, to appear flat with pigment alteration (mottling) in all eyes (including control) following dosing. Subretinal injection of vehicle control article was well tolerated and resulted in a procedure-related anterior segment inflammatory response that resolved by Day 15 and a mild to moderate posterior segment inflammatory response throughout the entire 9-month post dose observation period. In contrast, subretinal injection with AAV5-hGRK1-GUCY2D (GMP lot) resulted in a dose-dependent, severe anterior and posterior segment inflammatory response that generally peaked between Days 15 and 29. The anterior segment inflammation began to reduce in severity by Day 29 and resolved by Week 26 -30 in eyes administered 1.0 x 10^{12} or 4.0 x 10^{12} vg/mL and persisted through Week 39 in eyes administered 1.0 x 10^{13} or 4.9 x 10^{13} vg/mL. Dose-related posterior segment inflammation persisted through Week 39 at all dose levels of AAV5-hGRK1-GUCY2D and was characterized by varying degrees of vitreous cell, vitreous haze, white perivascular sheathing around retinal blood vessels, and subretinal to choroidal inflammatory foci within the injection site. Mottling of pigment in the RPE outside of the original subretinal injection bleb was sporadically observed in eyes administered 1.0 or 4.9 x10^{13} vg/mL and posterior synechia was observed in an eye administered 4.9 x 10^{13} vg/mL**.** Other than for an increased frequency of abnormally low IOP in eyes administered the viral vector, no clear and consistent difference was noted in IOP between groups.

OCT noted subretinal procedure- related findings of retinal detachment, accumulation of hyper-reflective material (HRM), and subretinal hyper-reflective material (SHRM) in the fovea, superiorly and at the edge of the bleb that persisted over time. While a variety of responses were noted within each dose level, the onset, incidence and severity of retinal degenerative changes were appreciated with increasing doses of AAV5-hGRK1-GUCY2D. Findings of an absent

bacillary layer, thinned or absent outer nuclear layer (ONL), choroidal disorganization and hyper-reflective foci (HF) and chorioretinal atrophy appeared earlier and more often with increasing dose levels. Findings of perivascular sheathing and retinal nerve fiber layer (RNFL) thickening, which are often associated with an inflammatory response, also appeared earlier and more frequently with increasing dose levels. Persistent inflammation noted on clinical ophthalmic examinations was consistent with the OCT findings.

Administration of AAV5-hGRK1-GUCY2D resulted in significantly reduced macular function (as assessed by mfERG) in eyes administered 1.0 x 10^{13} or 4.9 x 10^{13} vg/mL at Week 4 of the dosing phase. The mfERG of eyes administered lower dose levels of 1.0 x 10^{12} or 4.0 x 10^{12} vg/mL was less consistently affected at Week 4, although individual animals were affected. No consistent evidence of recovery was noted in the mfERG when tested at Weeks 12, 25 or 38 and, by Week 38, the lower dose levels of 1.0 x 10^{12} or 4.0 x 10^{12} vg/mL had progressed to include notably reduced macular function. For the scotopic ffERG, at Week 11 there was minor or no ERG depression at a dose level of 1.0 x 10^{12} vg/mL, some decrease in ffERG amplitude at 4.0 x 10^{12} vg/mL, and a marked depression of ffERG at 1.0 x 10^{13} or 4.9 x 10^{13} vg/mL. There was no evidence of recovery in the ffERG by Week 37, although two high dose females administered 4.9 x 10^{13} vg/mL with mfERG findings did not show depressed ffERGs, suggesting lesser extra-macular involvement in these females compared with males or other dose groups. The depression of retinal function in the foveal location in most animals by Week 38 implies a significant decrease in central visual function occurred in eyes of all AAV5-hGRK1-GUCY2D dose levels by 38 weeks post dose.

AAV5-hGRK1-GUCY2D-related microscopic observations were present at similar severity in all dose levels. Findings primarily affected the temporal posterior segment of the right eye in the area of the subretinal injection, and consisted of retinal degeneration/loss (disorganization, thinning, and/or loss of the photoreceptors, outer nuclear layer, outer plexiform layer, and

occasionally the inner nuclear layer), necrosis/loss of the retinal pigmented epithelium (RPE) cells, mononuclear cell inflammation, vitreous exudate, and decreased pigmentation in the remaining RPE cells. Minimal retinal vacuolation was also present in one male in each group administered AAV5-hGRK1-GUCY2D.

Adverse retinal findings seen via OCT included absent bacillary layer, thinned or absent outer nuclear layer, choroidal disorganization, persistent hyper-reflective foci, chorioretinal atrophy, perivascular sheathing and retinal nerve fiber layer thickening. The OCT retinal findings had adverse microscopic correlates of retinal degeneration/loss (disorganization, thinning, and/or loss of the photoreceptors, outer nuclear layer, outer plexiform layer, and occasionally the inner nuclear layer), necrosis/loss of the retinal pigmented epithelium cells, decreased pigmentation in the remaining RPE cells, mononuclear cell inflammation, and vitreous exudate. The OCT and microscopic retinal findings correlated with marked depression of retinal function by Week 38 as assessed by full-field and multi-focal electroretinography

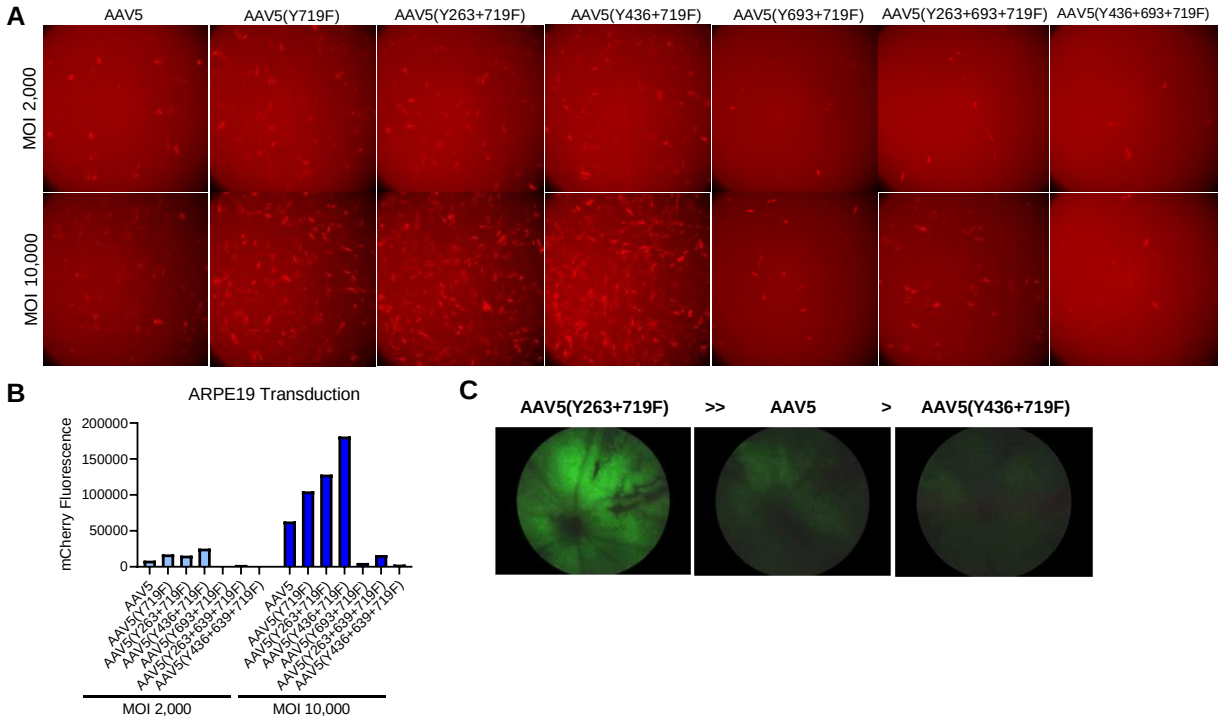

Figure S1. AAV5-based vectors containing self-complementary smCBA-mCherry genomes were tested for their relative transduction efficiency in APRE19 cells at low (2,000) or high (10,000) MOI. mCherry expression was captured with a fluorescent microscope (A) and transduction efficiency was quantified by flow cytometry (B). AAV5 and two AAV5-based capsid mutants containing hGRK1-GFP were selected for characterization subretinally injected mice. Fluorescent fundus images were taken to evaluate GFP expression at 1 month post-injection with vector at 1 x 10^{12} vg/mL (1 x 10^{9} vg/eye) (C).

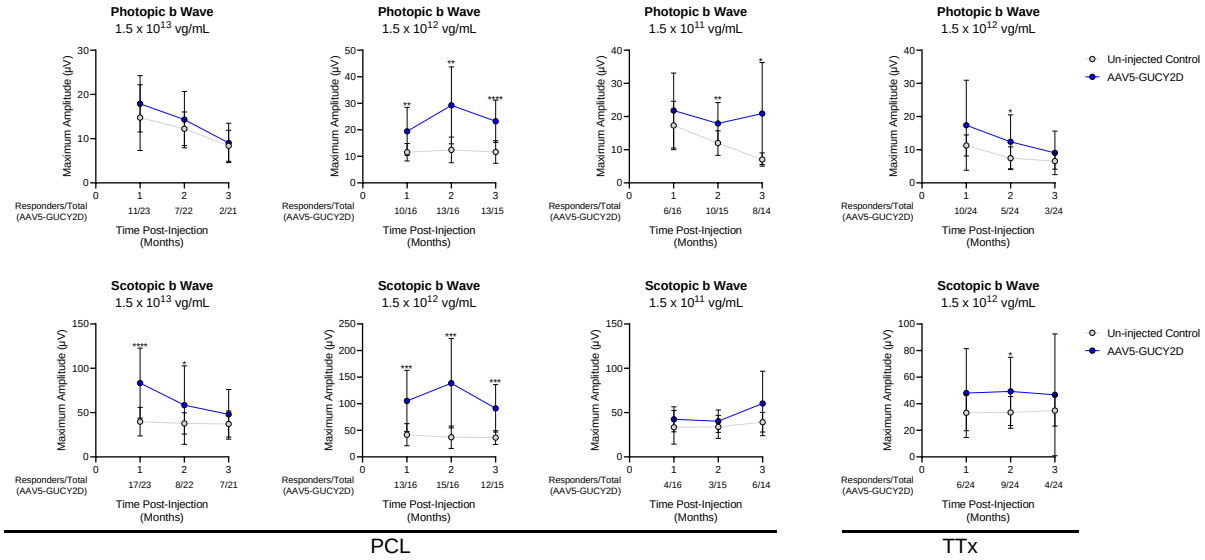

Figure S2. AAV5-hGRK1-GUCY2D produced via Producer Cell Line (PCL) or Triple Transfection (TTx) significantly improves retinal function in subretinally injected GCDKO mice. Cone-mediated (photopic, top row) and rod-mediated (scotopic, bottom row) function were evaluated in GCDKO mice for 3 months post injection with PCL-made vector at low (1.5 x 10^{11}vg/mL), mid (1.5 x 10^{12} vg/mL) or high (1.5 x 10^{13} vg/mL) concentrations, and with TTx-made vector at mid (1.5 x 10^{12} vg/mL) concentration. These correspond to doses of 1.5 x 10^{8}, 1.5 x 10^{9}, and1.5 x 10^{10} vg/eye, respectively. *p<0.05, **p<0.01, ***p<0.001, **** p>0.0001 as determined by multiple paired t tests with Holm-Sidak correction for multiple comparisons. The number of responders/total number of mice analyzed at each time point is reported on the X axis. Statistical analysis included all mice per cohort.

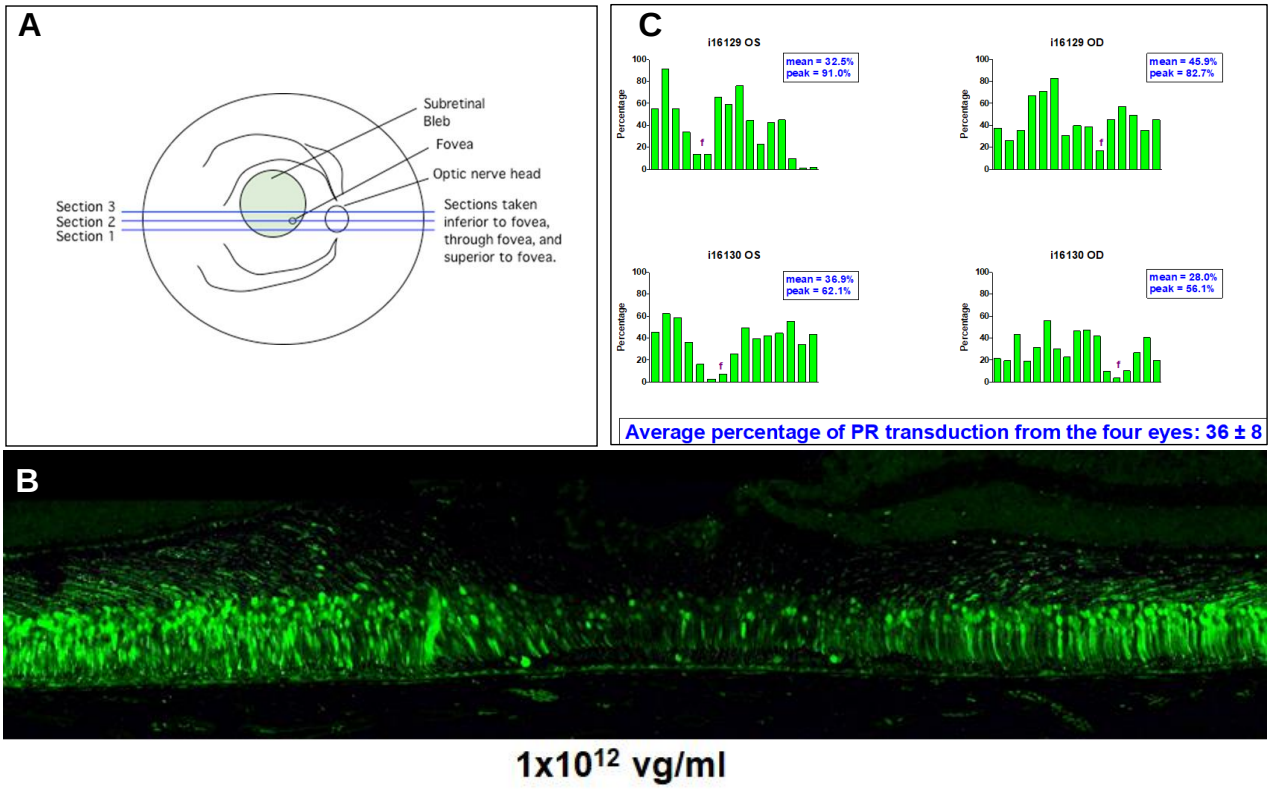

Figure S3. Schematic representation of how NHP sections were analyzed for GFP expression (A). Representative image of AAV5-hGRK1-mediated GFP expression in the foveal pit of cynomolgus macaque following subretinal injection at a concentration of 1 x 10^{12} vg/mL (1.2 x 10^{11} vg/eye) (B). Percentage of photoreceptors transduced following a subretinal administration of AAV5-hGRK1-eGFP at 3.3 x 10^{11} vg/mL (4.0 x 10^{10} vg/eye) in two NHPs, 4 eyes is shown to illustrate how quantification was performed (C).

Table S1- Study design for quantitatively evaluating photoreceptor mediated expression from AAV5-based capsid variants. AAV5 and two AAV5-based capsid variants containing either GFP or Gucy2e were subretinally delivered at low (1.0 x 10^{11} vg/mL) or high (1.0 x 10^{12} vg/mL) concentration. This corresponds to 1.0 x 10^{8} and 1.0 x 10^{9} vg/eye, respectively.

Group	Number of Animals Dosed	Test Article	Vector Dose		
			Volume	vg/mL	Total vg
1	12	AAV5-hGRK1-GFP	1 µL	1.0 x 10^{11}	1.0 x 10^{8}
2	13	AAV5-hGRK1-GFP	1 µL	1.0 x 10^{12}	1.0 x 10^{9}
3	13	AAV5(Y263+719F)-hGRK1-GFP	1 µL	1.0 x 10^{11}	1.0 x 10^{8}
4	12	AAV5(Y263+719F)-hGRK1-GFP	1 µL	1.0 x 10^{12}	1.0 x 10^{9}
5	12	AAV5(Y436+719F)-hGRK1-GFP	1 µL	1.0 x 10^{11}	1.0 x 10^{8}
6	12	AAV5(Y436+719F)-hGRK1-GFP	1 µL	1.0 x 10^{12}	1.0 x 10^{9}
7	20	AAV5-hGRK1-*Gucy2e*	1 µL	1.0 x 10^{11}	1.0 x 10^{8}
8	20	AAV5-hGRK1-*Gucy2e*	1 µL	1.0 x 10^{12}	1.0 x 10^{9}
9	20	AAV5(Y263+719F)-hGRK1-*Gucy2e*	1 µL	1.0 x 10^{11}	1.0 x 10^{8}
10	21	AAV5(Y263+719F)-hGRK1-*Gucy2e*	1 µL	1.0 x 10^{12}	1.0 x 10^{9}
11	19	AAV5(Y436+719F)-hGRK1-*Gucy2e*	1 µL	1.0 x 10^{11}	1.0 x 10^{8}
12	20	AAV5(Y436+719F)-hGRK1-*Gucy2e*	1 µL	1.0 x 10^{12}	1.0 x 10^{9}

Table S2- Quantification of titer in dose retains from the same vectors described in Table S1. TA= test article. Note that AAV5(Y263+719F)-hGRK1-GFP had a measured titer over 600 times greater than the expected titer. This discrepancy was considered when analyzing results.

Group	Test Article	Date of Test Article Preparation	Expected Titer (vg/mL)	Measured Titer (vg/mL)	% Recovery
1	AAV5-hGRK1-GFP	8-Sep-14	$1.0x10^{11}$	$1.76x10^{11}$	176
2	AAV5-hGRK1-GFP	25-Aug-14	$1.0x10^{12}$	$1.30x10^{12}$	130
2	AAV5-hGRK1-GFP	2-Sep-14	$1.0x10^{12}$	$1.17x10^{12}$	117
3	AAV5(Y263+719F)-hGRK1-GFP	30-Sep-14	$1.0x10^{11}$	$1.67x10^{11}$	169
4	AAV5(Y263+719F)-hGRK1-GFP	25-Aug-14	$1.0x10^{12}$	$6.69x10^{12}$	669
4	AAV5(Y263+719F)-hGRK1-GFP	2-Sep-14	$1.0x10^{12}$	$6.68x10^{12}$	668
5	AAV5(Y436+719F)-hGRK1-GFP	8-Sep-14	$1.0x10^{11}$	$1.34x10^{11}$	134
5	AAV5(Y436+719F)-hGRK1-GFP	11-Sep-14	$1.0x10^{11}$	$1.51x10^{11}$	151
6	AAV5(Y436+719F)-hGRK1-GFP	2-Sep-14	$1.0x10^{12}$	$7.74x10^{11}$	77.4
6	AAV5-hGRK1-Gucy2e	8-Sep-14	$1.0x10^{12}$	$1.04x10^{12}$	104
7	AAV5-hGRK1-Gucy2e	30-Sep-14	$1.0x10^{11}$	$1.85x10^{11}$	185
7	AAV5-hGRK1-Gucy2e	9-Oct-14	$1.0x10^{11}$	$1.99x10^{11}$	199
7	AAV5-hGRK1-Gucy2e	21-Oct-14	$1.0x10^{11}$	$1.67x10^{11}$	167
8	AAV5-hGRK1-Gucy2e	11-Jul-14	$1.0x10^{12}$	$1.40x10^{12}$	140
8	AAV5-hGRK1-Gucy2e	24-Jul-14	$1.0x10^{12}$	$1.52x10^{12}$	152
8	AAV5-hGRK1-Gucy2e	6-Aug-14	$1.0x10^{12}$	$1.40x10^{12}$	140
8	AAV5(Y263+719)-hGRK1-Gucy2e	20-Aug-14	$1.0x10^{12}$	$1.58x10^{12}$	158
9	AAV5(Y263+719)-hGRK1-Gucy2e	30-Sep-14	$1.0x10^{11}$	$1.05x10^{11}$	105
9	AAV5(Y263+719)-hGRK1-Gucy2e	9-Oct-14	$1.0x10^{11}$	$6.08x10^{11}$	60.8
9	AAV5(Y263+719)-hGRK1-Gucy2e	21-Oct-14	$1.0x10^{11}$	$1.29x10^{11}$	129
10	AAV5(Y263+719)-hGRK1-Gucy2e	6-Aug-14	$1.0x10^{12}$	$1.30x10^{11}$	130
10	AAV5(Y263+719)-hGRK1-Gucy2e	11-Jul-14	$1.0x10^{12}$	$1.20x10^{12}$	120
10	AAV5(Y263+719)-hGRK1-Gucy2e	20-Aug-14	$1.0x10^{12}$	$1.30x10^{12}$	130
11	AAV5(Y436+719F)-hGRK1-Gucy2e	9-Oct-14	$1.0x10^{11}$	$1.80x10^{12}$	180
11	AAV5(Y436+719F)-hGRK1-Gucy2e	21-Oct-14	$1.0x10^{11}$	$2.00x10^{11}$	200
12	AAV5(Y436+719F)-hGRK1-Gucy2e	20-Aug-14	$1.0x10^{12}$	$1.58x10^{12}$	158
12	AAV5(Y436+719F)-hGRK1-Gucy2e	25-Aug-14	$1.0x10^{12}$	$1.48x10^{12}$	148

Table S3. Study design for evaluating retinal function following subretinal delivery of AAV5-hGRK1-GUCY2D in GCDKO mice.

Group	Number of Animals Dosed (M/F)	Test Article	Vector Dose		
			Volume	vg/mL	Total vg
1	19 (13M/6F)	AAV5-hGRK1-*GUCY2D*	1 µL	1.5×10^{12}	1.5×10^{9}
2	22 (4M/18F)	AAV5-hGRK1-*GUCY2D*	1 µL	1.5×10^{13}	1.5×10^{10}

Table S4. Study design for evaluating retinal function following subretinal delivery of AAV5-GUCY2D, produced via triple transfection vs. producer cell line technology, in GCDKO mice. PCL = Producer Cell Line Manufactured, TTx = Triple Transfection Manufactured

Group	Number of Animals Dosed (M/F)	Test Article	Vector Dose		
			Volume	vg/mL	Total vg
1	25 (15M/10F)	AAV5-*GUCY2D* (PCL)	1 µL	1.5×10^{13}	1.5×10^{10}
2	16 (9M/7F)	AAV5-*GUCY2D* (PCL)	1 µL	1.5×10^{12}	1.5×10^{9}
3	16 (8M/8F)	AAV5-*GUCY2D* (PCL)	1 µL	1.5×10^{11}	1.5×10^{8}
4	34 (18M/16F)	AAV5-hGRK1-*GUCY2D* (TTx)	1 µL	1.5×10^{12}	1.5×10^{9}

Table S5. Hybrid study design for evaluating safety and efficacy following subretinal delivery of AAV5- GUCY2D to GC1KO mice. PCL = Producer Cell Line Manufactured

Group	Number of Animals Dosed (M/F)	Test Article	Vector Dose		
			Volume	vg/mL	Total vg
1	20 (14M/6F)	Vehicle	1 µL	N/A	N/A
2	36 (27M/9F)	AAV5-*GUCY2D* (PCL)	1 µL	3.3×10^{11}	3.3×10^{8}
3	41 (14M/27F)	AAV5-*GUCY2D* (PCL)	1 µL	1.5×10^{11}	1.5×10^{8}
4	17 (9M/8F)	AAV5-*GUCY2D* (PCL)	1 µL	3.3×10^{10}	3.3×10^{7}

Table S6. Study design for evaluating retinal function following subretinal delivery of AAV5-*Gucy2e* and AAV5-*GUCY2D* to GC1KO mice

Group	Number of Animals Dosed (M/F)	Test Article	Vector Dose		
			Volume	vg/mL	Total vg
1	21 (13M/8F)	AAV5-*GUCY2D*	1 µL	3.3×10^{11}	3.3×10^{8}
2	23 (15M/8F)	AAV5-*GUCY2D*	1 µL	1.0×10^{11}	1.0×10^{8}
3	18 (9M/9F)	AAV5-*GUCY2D*	1 µL	3.3×10^{10}	3.3×10^{7}
4	15 (9M/6F)	AAV5-*Gucy2e*	1 µL	3.3×10^{11}	3.3×10^{8}
5	22 (12M/10F)	AAV5-*Gucy2e*	1 µL	1.0×10^{11}	1.0×10^{8}
6	19 (7M/12F)	AAV5-*Gucy2e*	1 µL	3.3×10^{10}	3.3×10^{7}

Table S7- A statistical comparison of photopic (cone-mediated) function in GC1KO mice 1 month following subretinal injection of either AAV5-GUCY2D or AAV5-Gucy2e (study design in Table S6). Statistical comparisons across treatment groups were conducted using One-way Anova with Tukey's post-test. *p<0.05, **p<0.01, ***p<0.001, ****p<0.0001

Group		Statistical Significance							
		GUCY2D				*Gucy2e*			
		Un-injected	Hi	Med	Low	Un-injected	Hi	Med	Low
GUCY2D	Hi	****					n.s.	***	****
	Med	**	*				****	n.s.	*
	Low	n.s.	****	**			****	n.s.	n.s.
Gucy2e	Hi					****			
	Med					n.s.	****		
	Low					n.s	****	n.s.	

Table S8- A statistical comparison of photopic (cone-mediated) function in GC1KO mice 2 months following subretinal injection of either AAV5-GUCY2D or AAV5-Gucy2e (study design in Table S6). Statistical comparisons across treatment groups were conducted using One-way Anova with Tukey's post-test. *p<0.05, **p<0.01, ***p<0.001, ****p<0.0001

Group		Statistical Significance							
		GUCY2D				*Gucy2e*			
		Un-injected	Hi	Med	Low	Un-injected	Hi	Med	Low
GUCY2D	Hi	****					***	*	****
	Med	n.s.	n.s.				****	n.s.	n.s.
	Low	n.s.	****	n.s.			****	n.s.	n.s.
Gucy2e	Hi					****			
	Med					n.s.	****		
	Low					n.s	****	n.s.	

Table S9- A statistical comparison of photopic (cone-mediated) function in GC1KO mice 3 months following subretinal injection of either AAV5-GUCY2D or AAV5-Gucy2e (study design in Table S6). Statistical comparisons across treatment groups were conducted using One-way Anova with Tukey's post-test. *p<0.05, **p<0.01, ***p<0.001, ****p<0.0001

Group		Statistical Significance							
		GUCY2D				*Gucy2e*			
		Un-injected	Hi	Med	Low	Un-injected	Hi	Med	Low
GUCY2D	Hi	****					n.s.	*	****
	Med	n.s.	*				****	n.s.	n.s.
	Low	n.s.	****	n.s.			****	n.s.	n.s.
Gucy2e	Hi					****			
	Med					n.s.	****		
	Low					n.s	****	n.s.	

Table S10- A statistical comparison of scotopic (rod-mediated) function in GC1KO mice 1 month following subretinal injection of either AAV5-GUCY2D or AAV5-Gucy2e (study design in Table S6). Statistical comparisons across treatment groups were conducted using One-way Anova with Tukey's post-test. *p<0.05, **p<0.01, ***p<0.001, ****p<0.0001

Group		Statistical Significance							
		GUCY2D				*Gucy2e*			
		Un-injected	Hi	Med	Low	Un-injected	Hi	Med	Low
GUCY2D	Hi	n.s.					n.s.	**	n.s.
	Med	n.s.	n.s.				n.s.	**	n.s.
	Low	n.s.	n.s.	n.s.			n.s.	n.s.	n.s.
Gucy2e	Hi					n.s.			
	Med					n.s.	n.s.		
	Low					n.s	n.s.	**	

Table S11. Summary of photoreceptor (PR) transduction in NHP following a single subretinal administration of AAV5-hGRK1-eGFP. Both the average PR transduction across all eyes evaluated as well as the peak PR transduction across all eyes are reported.

Dose Level (vg/eye)	Concentration (vg/mL)	Number of Eyes	Average PR Transduction Per Group	Peak PR Transduction Across Eyes
1.2×10^{11}	1.0×10^{12}	8	51%	94.0%
8.0×10^{10}	6.7×10^{11}	4	50%	80.9%
4.0×10^{10}	3.3×10^{11}	4	36%	91.0%
1.2×10^{10}	1.0×10^{11}	8	4%	21.6%
4.0×10^{9}	3.3×10^{10}	4	0.6%	5.2%
1.2×10^{9}	1.0×10^{10}	4	0.3%	3.7%

Table S12. GLP study design to evaluate biodistribution of subretinally injected AAV5-GUCY2D in rats

Group No.	Test Article	Dose Level (vg/eye)[a]	Dose Conc. (vg/mL)	Number of Animals							
				Day 4 Necropsy		Day 15 (Week 3) Necropsy		Day 29 (Week 5) Necropsy		Day 92 (Month 3) Necropsy	
				M	F	M	F	M	F	M	F
1	Vehicle	0	0	2	2	2	2	2	2	2	2
2	AAV5-GUCY2D	2.0×10^{9}	1.0×10^{12}	5	5	5	5	5	5	5	5
3	AAV5-GUCY2D	2.0×10^{10}	1.0×10^{13}	5	5	5	5	5	5	5	5

M: Male, F: female, Conc: concentration

[a]: Unilateral subretinal injection at a dose volume of 2 mL/right eye/animal. The left eye of each animal served as an untreated control

Table S13. Summary of AAV5-GUCY2D vector DNA concentrations in tissues and fluids from rats subretinally injected with the low dose (2.0 x 10^9 vg/eye; Group 2 in Table S12)

Summary AAV5-GUCY2D Vector DNA Concentrations in Group 2 Tissues and Fluids

	Group 2							
	Day 4		Day 15		Day 29		Day 92	
Sample Type	Conc	N	Conc	N	Conc	N	Conc	N
Blood	<LLOQ	0/10	<LLOQ	0/10	-	-	-	-
Brain-FB-Left	<LLOQ	0/10	168.57 to 193.01	2/10	43.44 to 422.17	5/10	45.14 to 53.36	2/10
Brain-FB-Right	<LLOQ	0/10	<LLOQ	0/10	-	-	-	-
Brain-NVC-Left	44.49 to 46.71	2/10	48.89 to 497.34	2/10	37.10 to 624.20	6/10	37.44 to 153.20	3/10
Brain-NVC-Right	<LLOQ	0/10	<LLOQ	0/10	-	-	-	-
Diaphragm	53.61 to 98.49	3/10	<LLOQ	0/10	<LLOQ	0/10	-	-
Eye-Untreated	<LLOQ	0/10	<LLOQ	0/10	-	-	-	-
Eye-Treated (right)	390941.39 to 1656975.66	10/10	197519.07 to 1478457.85	10/10	28776.31 to 2163739.12	10/10	10885.89 to 949049.61	10/10
Heart	<LLOQ	0/10	<LLOQ	0/10	-	-	-	-
Kidney	37.29 to 79.46	4/10	44.8	1/10	33.60	1/10	<LLOQ	0/10
LN Mandibular	47.19 to 3709.17	10/10	45.33 to 179.14	4/10	36.59 to 108.61	2/10	54.73 to 69.37	2/10
Liver	65.26 to 898.66	9/10	46.24 to 243.04	5/10	<LLOQ	0/10	<LLOQ	0/10
Lung	51.43 to 338.87	9/10	32.06 to 218.19	5/10	47.33 to 84.99	2/10	<LLOQ	0/10
Muscle	<LLOQ	0/10	<LLOQ	0/10	-	-	-	-
ONU*	<LLOQ	0/10	6320.87	1/10	1177.04	1/10	<LLOQ	0/10
ONT* (right)	705.53 to 2637.07	5/10	991.35 to 16360.66	4/10	4133.33 to 35015.16	4/10	1677.95 to 2923.20	4/10
Ovary	81.86 to 96.83	3/5	<LLOQ	0/5	<LLOQ	0/5	-	-
Spleen	90.37 to 1539.41	10/10	61.00 to 476.26	7/10	66.34 to 1055.39	2/10	49.46 to 160.13	2/10
Testes	68.33	1/5	<LLOQ	0/5	< LLOQ	0/5	-	-

LLOQ = Lower Limit of Quantitation: 25 copies/reaction; - = tissues not analysed as two consecutive negative postdose qPCR results were obtained

Conc. = Concentration of GUCY2D (copies/µg DNA); N = Number of Animals with Signal >LLOQ / Number of Animals Tested

FB = Forebrain; NVC = Near Visual Cortex; ONT = Optic Nerve from treated eye; ONU = Optic Nerve from untreated eye

Table S14. Summary of AAV5-GUCY2D vector DNA concentrations in tissues and fluids from rats subretinally injected with the high dose (2.0 x 10^{10} vg/eye; Group 3 from Table S12)

Summary AAV5-GUCY2D Vector DNA Concentrations in Group 3 Tissues and Fluids

	Group 3							
	Day 4		Day 15		Day 29		Day 92	
Sample Type	Conc	N	Conc	N	Conc	N	Conc	N
Blood	550.00 to 3952.04	6/10	<LLOQ	0/10	< LLOQ	0/10	< LLOQ	0/10
Brain-FB-Left	62.81	1/10	137.79 to 1812.20	4/10	48.59 to 62.03	4/10	35.69	1/10
Brain-FB-Right	<LLOQ	0/10	62.1	1/10	< LLOQ	0/10	< LLOQ	0/10
Brain-NVC-Left	67.31 to 271.54	5/10	74.91 to 2727.79	8/10	153.36 to 361.51	5/10	< LLOQ	0/10
Brain-NVC-Right	<LLOQ	0/10	<LLOQ	0/10	-	-	-	-
Diaphragm	126.17 to 4587.77	6/10	288.81	1/10	< LLOQ	0/10	< LLOQ	0/10
Eye-Untreated	39.06 to 90.04	3/10	49.01	1/10	< LLOQ	0/10	< LLOQ	0/10
Eye-Treated (right)	961036.39 to 13556646.54	10/10	859882.40 to 9333341.91	10/10	145796.13 to 1292278.86	10/10	10042.24 to 246133.04	10/10
Heart	56.16 to 277.01	5/10	60.73	1/10	< LLOQ	0/10	< LLOQ	0/10
Kidney	38.64 to 1170.50	8/10	534.97	1/10	51.63 to 249.84	4/10	< LLOQ	0/10
LN Mandibular	153.84 to 5216.84	10/10	115.81 to 3170.21	10/10	49.76 to 1706.59	10/10	151.30 to 2304.06	6/10
Liver	378.11 to 34430.57	10/10	48.54 to 2629.84	9/10	37.11 to 110.31	3/10	< LLOQ	0/10
Lung	116.76 to 5189.30	10/10	50.96 to 1744.11	8/10	40.44 to 1114.01	8/10	38.46 to 50.70	2/10
Muscle	52.87 to 68.27	2/10	<LLOQ	0/10	< LLOQ	0/10	-	-
ONU*	<LLOQ	0/10	1341.05 to 2193.71	2/10	< LLOQ	0/10	< LLOQ	0/10
ONT* (right)	1828.63 to 75432.80	9/10	3288.33 to 121612.20	10/10	3141.86 to 13576.67	5/10	1646.22 to 2543.11	2/10
Ovary	62.47 to 1092.24	5/5	<LLOQ	0/5	41.14 to 53.01	2/5	< LLOQ	0/5
Spleen	514.36 to 28235.64	10/10	66.21 to 8562.81	10/10	45.66 to 1071.41	9/10	282.21	1/10
Testes	92.30 to 144.80	2/5	135.33	1/5	59.30	1/5	< LLOQ	0/5

LLOQ = Lower Limit of Quantitation: 25 copies/reaction; - = tissues not analysed as two consecutive negative postdose qPCR results were obtained

Conc. = Concentration of GUCY2D (copies/µg DNA); N = Number of Animals with Signal >LLOQ / Number of Animals Tested

FB = Forebrain; NVC = Near Visual Cortex; ONT = Optic Nerve from treated eye; ONU = Optic Nerve from untreated eye

Table S15. Quantification of biodistribution (presence of vector genomes) in retinas (within and outside the injection bleb) of NHPs dosed in GLP Tox Study #1 (Mean Log_{10}GUCY2D copies/µg RNA).

Tissue	Timepoint	Dose Level (vg/mL)				
		0	1.0 x 10^{12}	4.0 x 10^{12}	1.0 x 10^{13}	4.9 x 10^{13}
Retinal punch (bleb area)	Day 29	1.0[a]	6.6	6.7	7.0[b]	6.7
Retinal Punch (non bleb area)	Day 29	1.0[a]	1.5	3.1	1.8[b]	3.4

[a] Equivalent to all samples <LLOQ.

Table S16. Quantification of biodistribution (presence of vector genomes) in remaining tissues and blood of NHPs dosed in GLP Tox Study #1 (Group Mean Copies/μg DNA)

Tissue	Timepoint	Sex	Dose Level (vg/mL)				
			0	$1.0x10^{12}$	$4.0x10^{12}$	$1.0x10^{13}$	$4.9x10^{13}$
Blood- DNA	Predose 1	M	<LLOQ	<LLOQ	<LLOQ	<LLOQ	<LLOQ
		F	<LLOQ	<LLOQ	<LLOQ	<LLOQ	<LLOQ
	Predose 2	M	<LLOQ	<LLOQ	<LLOQ	<LLOQ	<LLOQ
		F	<LLOQ	<LLOQ	<LLOQ	<LLOQ	<LLOQ
	Week 2	M	<LLOQ	179.74	765.01	764.16	1367.47
		F	<LLOQ	481.64	585.09	1326.54	17437
	Week 5	M	<LLOQ	<LLOQ	55.84	58.77	205.53
		F	<LLOQ	<LLOQ	<LLOQ	70.24	969
	Week 9	M	NA	<LLOQ	<LLOQ	<LLOQ	151.64
		F	NA	<LLOQ	<LLOQ	<LLOQ	792.23
	Week 13	M	NA	NA	<LLOQ	<LLOQ	<LLOQ
		F	NA	NA	<LLOQ	<LLOQ	444.73
	Week 17	M	NA	NA	NA	NA	<LLOQ
		F	NA	NA	NA	NA	<LLOQ
	Week 21	M	NA	NA	NA	NA	<LLOQ
		F	NA	NA	NA	NA	<LLOQ
	Week 26	M	NA	NA	NA	NA	NA
		F	NA	NA	NA	NA	<LLOQ
Brain (Right Occipital Lobe)	Day 29	M	<LLOQ	2585.76	938.04	1322.69	971.72
		F	<LLOQ	1472.69	885.79	826.79	1996.13
Brain (Left Occipital Lobe)	Day 29	M	<LLOQ	510.04	776.41	185.29	462.88
		F	<LLOQ	631.56	223.69	176.37	791.74
Optic Nerve (Right)	Day 29	M	<LLOQ	48449.63	9423.44	20728.11	<LLOQ
		F	<LLOQ	<LLOQ	64037.9	<LLOQ	3393.5
Spleen	Day 29	M	<LLOQ	3487.01	209.54	2301.24	2346.26
		F	<LLOQ	71.94	972.26	54545.4	27021.98
Liver	Day 29	M	<LLOQ	273.33	<LLOQ	69.91	55.71
		F	<LLOQ	<LLOQ	67.04	3657.13	252.23

Note: LLOQ for blood samples = 36 copies/μg/DNA. For calculation purposes <LLOQ was assigned as LLOQ/2 (18 copies/μg DNA)
NA = Not analyzed

Table S17. Summary of Anti-AAV5 antibodies present in serum and aqueous humor of NHPs subretinally injected in GLP Tox Study #1. Concentrations of 1.0 x 10^{12}, 4.0 x 10^{12}, 1.0 x 10^{13}, and 4.9 x 10^{13} vg/mL were delivered in 150 μL, corresponding to 1.5 x10^{11}, 6.0 x 10^{11}, 1.5 x 10^{12}, and 7.4 x 10^{12} vg/eye, respectively.

Number of Animals with *Serum* Anti-AAV5 Antibodies					
Timepoint	**Dose Level (vg/mL)**				
	0	1.0 x 10^{12}	4.0 x 10^{12}	1.0 x 10^{13}	4.9 x 10^{13}
Predose 1	0 of 8	1 of 8	0 of 8	3 of 8	4 of 8
Predose 2	0 of 8	1 of 8	0 of 8	2 of 8	4 of 8
Week 2	0 of 8	1 of 8	4 of 8	7 of 8	8 of 8
Week 5	0 of 8	7 of 8	8 of 8	8 of 8	8 of 8
Week 9	0 of 4	4 of 4	4 of 4	4 of 4	4 of 4
Week 13	0 of 4	4 of 4	4 of 4	4 of 4	4 of 4
Week 17	0 of 4	4 of 4	4 of 4	4 of 4	4 of 4
Week 21	0 of 4	4 of 4	4 of 4	4 of 4	4 of 4
Week 26	1 of 4	4 of 4	4 of 4	4 of 4	4 of 4
Week 30	1 of 4	4 of 4	4 of 4	4 of 4	4 of 4
Week 34	1 of 4	4 of 4	4 of 4	4 of 4	4 of 4
Week 39	0 of 4	4 of 4	4 of 4	4 of 4	4 of 4

Number of Animals with *Aqueous* Anti-AAV5 Antibodies					
Timepoint	**Dose Level (vg/mL)**				
	0	1.0 x 10^{12}	4.0 x 10^{12}	1.0 x 10^{13}	4.9 x 10^{13}
Predose	0 of 8	0 of 8	0 of 8	0 of 8	0 of 8
Interim Necropsy	0 of 8	4 of 4	4 of 4	4 of 4	4 of 4
Terminal Necropsy	0 of 4	4 of 4	4 of 4	4 of 4	4 of 4

Table S18. Bridging study design for evaluating the effects of two lots of AAV5-GUCY2D (vector from the GLP Tox study vs. the GMP clinical candidate) on retinal function in subretinally injected GC1KO mice

Group	Number of Animals Dosed (M/F)	Test Article	Lot	Dose Volume	Dose Concentration (vg/mL)	Dose (vg/eye)
1	20 (9M/11F)	AAV5-*GUCY2D*	Tox Lot	1 µL into one eye	1.5×10^{11}	1.5×10^{8}
2	20 (11M/9F)				3.3×10^{10}	3.3×10^{7}
3	20 (8M/12F)		GMP Lot		1.5×10^{11}	1.5×10^{8}
4	21 (12M/9F)				3.3×10^{10}	3.3×10^{7}

Table S19. Preclinical Data Summary informs dose selection in Phase I/II clinical trials. NOAEL= No observable adverse effect level, MED= minimum effective dose

Dose Concentration (vg/mL)	GCDKO/GC1KO Mouse Studies	NHP Pharmacology Studies (peak % transduction)	GLP Toxicology
1.0×10^{13}	Efficacy/ Toxicity (↓ONL by OCT)	Not done	
1.0×10^{12}	Efficacy GCDKO	94% PR transduction	NOAEL
6.7×10^{11}	Not done	81% PR transduction	
3.3×10^{11}	Efficacy GC1KO	91% PR transduction	
1.0×10^{11}	Efficacy GCDKO/ Efficacy GC1KO	22% PR transduction	
3.3×10^{10}	Efficacy GC1KO	5% PR transduction	MED
1.0×10^{10}	Not done	4% PR transduction	

Table S20. Summary of *in vivo* experiments conducted in this study

Description of Study	Study Design Table	Animal model	Test/control article used	concentration (vg/mL)	dose (vg/eye)	# of animals dosed (M/F)	Statitistics employed
Compare PR transduction and ERG improvements following subretinal injection of AAV5-based vectors containing GFP or Gucy2e, respectively	**Table S1**	GCDKO mouse	AAV5-hGRK1-GFP	1×10^{11}	1×10^{8}	12	stats performed on ERG data (**Figure 1**) using one-way ANOVA with Tukey's post-test analysis
			AAV5-hGRK1-Gucy2e			20	
			AAV5(Y263+719)-hGRK1-GFP			13	
			AAV5(Y263+719)-hGRK1-Gucy2e			20	
			AAV5(Y436+719)-hGRK1-GFP			12	
			AAV5(Y436+719)-hGRK1-Gucy2e			19	
			AAV5-hGRK1-GFP	1×10^{12}	1×10^{9}	13	
			AAV5-hGRK1-Gucy2e			20	
			AAV5(Y263+719)-hGRK1-GFP			12	
			AAV5(Y263+719)-hGRK1-Gucy2e			21	
			AAV5(Y436+719)-hGRK1-GFP			12	
			AAV5(Y436+719)-hGRK1-Gucy2e			20	
Evaluate efficacy of AAV5 containing human GUCY2D	**Table S3**	GCDKO mouse	AAV5-hGRK1-GUCY2D	1.5×10^{12}	1.5×10^{9}	19 (13M/6F)	stats performed on ERG data (**Figure 2**) using multiple paired t tests with Holm-Sidak correction for multiple comparisons.
				1.5×10^{13}	1.5×10^{10}	22 (4M/18F)	
Compare efficacy of AAV5-hGRK1-GUCY2D vectors manufactured via producer cell line (PCL) vs. triple transfection (TTx) process	**Table S4**	GCDKO mouse	AAV5-hGRK1-GUCY2D (PCL)	1.5×10^{11}	1.5×10^{8}	16 (8M/8F)	stats performed on ERG data (**Figure S2)** using multiple paired t tests with Holm-Sidak correction for multiple comparisons. Stats performed on ERG data (**Figure 3**) using two-way ANOVA with Sidak's post-test analysis. Stats performed on OCT data (Figure 3) using two-way ANOVA with Tukey's post-test
				1.5×10^{12}	1.5×10^{9}	16 (9M/7F)	
				1.5×10^{13}	1.5×10^{10}	25 (15M/10F)	
			AAV5-hGRK1-GUCY2D (TTx)	1.5×10^{12}	1.5 x 109	34 (18M/16F)	
Hybrid study evaluating AAV5-hGRK1-GUCY2D	**Table S5**	GC1KO mouse	AAV5-hGRK1-GUCY2D	3.3×10^{10}	3.3×10^{7}	17 (9M/8F)	stats performed on ERG and OCT data (**Figure 4**) using by two-way ANOVA with Tukey's post-test analysis.
				1.5×10^{11}	1.5×10^{8}	41 (14M/27F)	
				3.3×10^{11}	3.3×10^{8}	36 (17M/9F)	
			Vehicle	N/A	N/A	20 (14M/6F)	
Compare therapeutic response to AAV5 vectors containing murine Gucy2e vs.human GUCY2D	**Table S6**	GC1KO mouse	AAV5-hGRK1-GUCY2D	3.3×10^{10}	3.3×10^{7}	18 (9M/9F)	stats performed on ERG data (**Table S7, S8, S9, S10 and Figure 5**) using (need this info from Dana). Stats performed on OCT data (**Figure 5**) using two-way ANOVA with Tukey's post-test analysis
			AAV5-hGRK1-GUCY2D	1.0×10^{11}	1.0×10^{8}	23 (15M/8F)	
			AAV5-hGRK1-GUCY2D	3.3×10^{11}	3.3×10^{8}	21 (13M/8F)	
			AAV5-hGRK1-Gucy2e	3.3×10^{10}	3.3×10^{7}	19 (7M/12F)	
			AAV5-hGRK1-Gucy2e	1.0×10^{11}	1.0×10^{8}	22 (12M/10F)	
			AAV5-hGRK1-Gucy2e	3.3×10^{11}	3.3×10^{8}	15 (9M/6F)	
Evaluate photoreceptor transduction in subretinally injected NHPs	**Table S11**	cynomolgus macaque	AAV5-hGRK1-GFP	1.0×10^{10}	1.2×10^{9}	2	N/A
				3.3×10^{10}	4.0×10^{9}	2	
				1.0×10^{11}	1.2×10^{10}	4	
				3.3×10^{11}	4.0×10^{10}	2	
				6.7×10^{11}	8.0×10^{10}	2	
				1.0×10^{12}	1.2×10^{11}	4	
GLP rat biodistribution study	**Table S12**	Long Evans rats	AAV5-hGRK1-GUCY2D	1.0×10^{12}	2.0×10^{9}	40 (20M/20F)	N/A
				1.0×10^{13}	2.0×10^{10}	40 (20M/20F)	
			Vehicle	N/A	N/A	16 (8M/8F)	
GLP NHP Safety Study #1	**Table 1**	cynomolgus macaque	AAV5-hGRK1-GUCY2D	1.0×10^{12}	1.5×10^{11}	8 (4M/4F)	N/A
				4.0×10^{12}	6.0×10^{11}	8 (4M/4F)	
				1.0×10^{13}	1.5×10^{12}	8 (3M/4F)	
				4.9×10^{13}	7.4×10^{12}	8 (4M/4F)	
			Vehicle	N/A	N/A	8 (4M/4F)	
GLP NHP Safety Study #2	**Table 2**	cynomolgus macaque	AAV5-hGRK1-GUCY2D[a]	1.0×10^{11}	1.5×10^{10}	3F	N/A
				3.3×10^{11}	5.0×10^{10}	3F	
				1.0×10^{12}	1.5×10^{11}	3F	
			Vehicle[a]	N/A	N/A	3F	
			AAV5-hGRK1-GUCY2D[b]	1.0×10^{11}	1.5×10^{10}	3F	
				3.3×10^{11}	5.0×10^{10}	3F	
				1.0×10^{12}	1.5×10^{11}	3F	
			Vehicle[b]	N/A	N/A	3F	
Evaluate comparability between Tox lot vs.GMP test articles	**Table S18**	GC1KO mice	AAV5-hGRK1-GUCY2D (Tox lot)	3.3×10^{10}	3.3×10^{7}	20 (11M/9F)	stats performed on ERG data (**Figure 6**) using by one-way ANOVA with Tukey's post-test analysis. Stats performed on OCT data (**Figure 6**) using two-way ANOVA with Tukey's post-test analysis
				3.3×10^{11}	3.3×10^{8}	20 (9M/11F)	
			AAV5-hGRK1-GUCY2D (GMP lot)	3.3×10^{10}	3.3×10^{7}	21 (12M/9F)	
				3.3×10^{11}	3.3×10^{8}	20 (8M/12F)	

[a]- mild steroid reigmen, [b]- moderate steroid regimen